Journal Pre-proofs

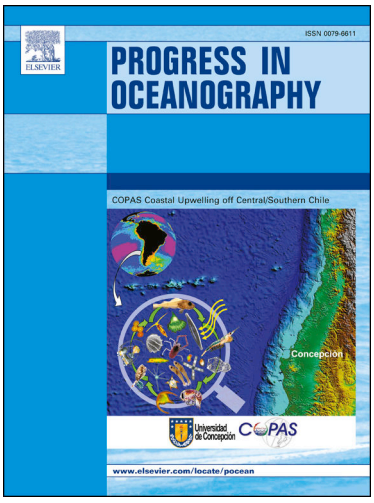

Sediment dynamics in the Gulf of Lion (NW Mediterranean Sea) during two autumn-winter periods with contrasting meteorological conditions

Claude Estournel, Guillaume Mikolajczak, Caroline Ulses, François Bourrin, Miquel Canals, Sabine Charmasson, David Doxaran, Thomas Duhaut, Xavier Durrieu de Madron, Patrick Marsaleix, Albert Palanques, Pere Puig, Olivier Radakovitch, Anna Sanchez-Vidal, Romaric Verney

PII: S0079-6611(22)00201-4
DOI: https://doi.org/10.1016/j.pocean.2022.102942
Reference: PROOCE 102942

To appear in: *Progress in Oceanography*

Received Date: 16 February 2022
Revised Date: 4 September 2022
Accepted Date: 8 December 2022

Please cite this article as: Estournel, C., Mikolajczak, G., Ulses, C., Bourrin, F., Canals, M., Charmasson, S., Doxaran, D., Duhaut, T., Durrieu de Madron, X., Marsaleix, P., Palanques, A., Puig, P., Radakovitch, O., Sanchez-Vidal, A., Verney, R., Sediment dynamics in the Gulf of Lion (NW Mediterranean Sea) during two autumn-winter periods with contrasting meteorological conditions, *Progress in Oceanography* (2022), doi: https://doi.org/10.1016/j.pocean.2022.102942

Sediment dynamics in the Gulf of Lion (NW Mediterranean Sea) during two autumn-winter periods with contrasting meteorological conditions

Claude Estournel[1,*], Guillaume Mikolajczak[1], Caroline Ulses[1], François Bourrin[2], Miquel Canals[3], Sabine Charmasson[4], David Doxaran[5], Thomas Duhaut[1], Xavier Durrieu de Madron[2], Patrick Marsaleix[1], Albert Palanques[6], Pere Puig[6], Olivier Radakovitch[4], Anna Sanchez-Vidal[3], Romaric Verney[7]

(1) LEGOS, Université de Toulouse, CNES/CNRS/IRD/UT3, 14 avenue Edouard Belin, 31400 Toulouse, France
(2) CEFREM, CNRS, Université de Perpignan Via Domitia, 52 Avenue Paul Alduy, 66860 Perpignan, France
(3) GRC, Marine Geosciences, Department of Earth and Marine Dynamics, Faculty of Earth Sciences, University of Barcelona, Martí i Franquès s/n, E-08028 Barcelona, Spain
(4) Institut de Radioprotection et de Sûreté Nucléaire (IRSN), PSE-ENV/SRTE/LRTA, BP 13, F-13115 Saint-Paul-Les-Durance, France
(5) LOV, Sorbonne Université, CNRS, 181 Chemin du Lazaret, 06230 Villefranche-sur-Mer, France
(6) Marine Sciences Institute, Consejo Superior de Investigaciones Científicas, Barcelona 08003, Spain
(7) IFREMER, DYNECO/DHYSED, ZI Pointe du Diable, 29280 Plouzané, France

* Corresponding author
LEGOS/OMP 14 avenue Edouard Belin, 31400 Toulouse, France
email: claude.estournel@legos.obs-mip.fr

Highlights

- Strong interannual variability of the sediment dynamics in the Gulf of Lion
- Massive sediment accumulation near the Rhone River mouth (~ 56% of the river inputs)
- Sediment deficit on the inner shelf due to the long-term reduction of the Rhone inputs
- Storm-induced sediment accumulation in the southwestern Gulf of Lion
- Cold winters mainly impact the southwestern and outer shelf and the submarine canyons

Abstract
A simulation based on a hydro-sedimentary model was conducted for the period between summer 2010 and spring 2012 in the Gulf of Lion (northwestern Mediterranean Sea) to understand the spatial and temporal variability of sediment transport, erosion and deposition on the continental shelf and slope. Datasets of both simulated and observed current, temperature and suspended matter from the shelf and the Cap de Creus Canyon which is the main export route towards the continental slope, were first compared to assess the reliability of the simulation. The simulation shows the massive sediment accumulation near the Rhone River mouth (~ 56% of the inputs), the accretion along the mid-shelf mud belt, and the impact of dense shelf water cascading on sediment resuspension and erosion inside the Cap de Creus Canyon. The two studied autumn-winter periods were strongly contrasted in terms of meteorological conditions and subsequent impacts on the sediment dynamics. During the first period (2010–2011) dominated by marine storms, the shelf sediment underwent strong changes, the Rhone River sediment load accumulated in a relatively small area, stock of littoral sands moved to the inner shelf (20–40 m) while inner shelf fine particles fed the mid-shelf mud belt and the upper Cap de Creus Canyon. During the second period (2011–2012) with very little marine wind and a particularly cold winter, sediment on the shelf underwent little change except for a southwestward growth of the Rhone River prodeltaic deposit. Sediment from the southwestern end of the shelf as

well as from the upper Cap de Creus Canyon was flushed toward deeper reaches by dense shelf water cascading. Cascading also had a more moderate impact in the various canyons incising the continental shelf. Our work supports the view of an unbalanced sedimentary system, with a deficit mainly over the inner shelf, whose main driver is probably the strong and fast reduction of particulate matter inputs from the Rhone River (by a factor of 4 in less than one century).

Keywords
Sediment transport, continental shelf, submarine canyons, storms, cascading, flood, northwestern Mediterranean Sea, Gulf of Lion, Rhone River

Graphical abstract

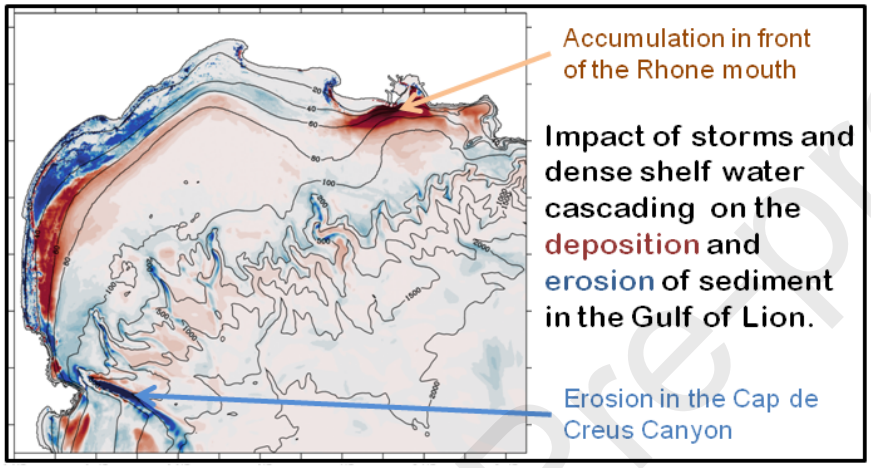

1. Introduction

One of the complexities of sediment dynamics of continental shelves arises from the multiplicity of temporal scales involved. The 120 m sea level rise that occurred between 21,000 and 6,000 years ago set the shifting boundaries and extent of continental shelves. Sediment input by rivers then shaped deltas, estuaries, coastal prisms and mud belts on the shelves. The growing anthropogenic influence on terrestrial environments, rivers and coasts induced changes in sediment transport and accumulation, which accelerated from the end of the 19th century. On a shorter time scale, we are able to identify the most visible impacts of extreme events, such as floods and storms, resulting for instance in the silting of estuaries or the retreat of the coastline. Finally, it is likely that climate change already has an impact on sediment dynamics. In the Mediterranean region, the frequency of heat waves and droughts is increasing (Tramblay and Somot, 2018), as are extreme precipitation events (Lionello et al., 2008) that cause catastrophic floods and drive impulsive sediment inputs to the sea.

While sedimentation rates and budgets classically derived from dated sediment cores allow evaluating the long-term sedimentation patterns (i.e. centuries to decades), these approaches do not allow quantifying the impact of specific events such as a flood or a storm, neither the cumulated effects of several such events on seasonal and interannual scales. The objective of this study, based on numerical modelling, is to fill the knowledge gap on the high frequency sediment dynamics in the Gulf of Lion shelf, NW Mediterranean Sea, ranging from individual meteo-oceanic events to interannual time scales.

The following subsections in this Introduction provide background information on the study site, the characteristics of surficial deposits, the long-term sedimentation rates, the hydrologic and meteorological context, and the identified impacts of a whole set of drivers on sediment erosion, transport and deposition.

Physiography and sediment cover

The Gulf of Lion continental margin in the northwestern Mediterranean Sea encompasses the outlet of the Rhone River and a vast crescent shaped continental shelf, 75 km wide in its center, which opens to a continental slope incised by numerous submarine canyons (Fig. 1). To the southwest, the shelf ends against the Cap de Creus promontory where the head of the canyon with the same name is at 4 km from the coast only. This canyon has been identified as the main pathway for sediment transfer from the shelf to the slope and deep basin (Canals et al., 2006; Ulses et al., 2008a; Palanques et al., 2012).

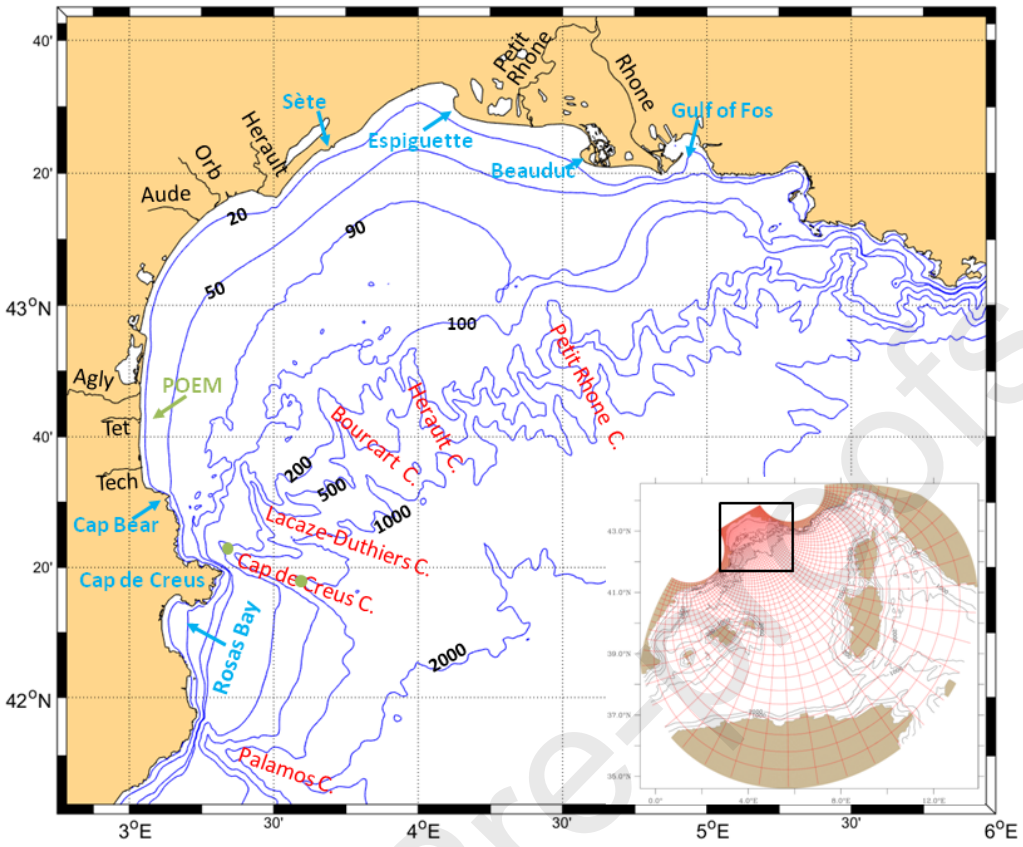

Figure 1. Bathymetry of the Gulf of Lion (blue lines). The main rivers considered in the model are in black, the places cited in the text in blue and the main submarine canyons in red. The observation sites are indicated in green: the POEM buoy station and the filled circles representing the two moorings in the Cap de Creus Canyon at 300 and 1000 m depth. The insert represents the bipolar grid of the SYMPHONIE simulation (1 point out 10 is represented) with the black square being the Gulf of Lion.

In areas beyond the direct influence of rivers, the inner shelf is defined by a sand-covered seafloor that extends down to 30 m depth. From that depth down to 80-90 m, an increase of silt and clay is observed thus forming the well- known “mid shelf mud belt”. Deeper than this and down to 120-135 m, the outer shelf consists of relict littoral sands of the Last Glacial Maximum with paleo-shorelines of the subsequent transgression (Got and Aloısi, 1990; Berné et al., 2004, Bassetti et al., 2006). These relict sands are covered by a thin layer of mud (Bassetti et al., 2006).

The Rhone mean annual water discharge is around 1,700 $m^3\ s^{-1}$ and varies from a few hundred $m^3\ s^{-1}$ at low water level to around 6,000 $m^3\ s^{-1}$ for a flood with a return period of 2 years, to about 11, 000 $m^3\ s^{-1}$ for a centennial return flood (Pont et al., 2002). South of Arles (50 km upstream from the river mouth), it splits into two channels, the Grand Rhone to the east encompassing 90% of the total discharge and the Petit Rhone to the west with the remaining 10%. The Rhone mean solid suspended discharge is estimated between 6.6 and 8.4 Mt/year (Pont et al., 2012; Sadaoui et al., 2016; Poulier et al., 2019) with a strong interannual variability (from 2.2 to 18 Mt/year according to Poulier et al., 2019). These inputs would have decreased considerably (by a factor of 4) compared to the period covering the 19th century and first half of the 20th century (Sabatier et al., 2006), due to a decrease in flood frequency and anthropogenic factors (changes in land use, reforestation, dams, dredging, Provansal et al., 2014).

The Grand Rhone River mouth (called Rhone thereafter for simplicity) is located in a microtidal context influenced mainly by waves and associated currents (Maillet et al., 2006). The region has the morpho-sedimentary characteristics of a delta with a mouth bar located less than 2 km from the

mouth and extending from the coastline to 4 m depth, followed by the delta front characterized by a strong slope (~ 4°) between 4 and 20 m depth and then the prodelta characterized by a lower slope. The delta front advances seawards by progradation under the effect of massive sediment deposition (Sabatier et al., 2006, Maillet et al., 2006) while the sediment accumulation on the prodelta is less. Beyond the sand mouth bar, sediments in the deltaic zone are mainly thin layered silty muds, with a fine fraction increasing rapidly seawards between 30 and 60 m of water depth as a result of selective deposition (Chassefière, 1990). Like most authors dealing with sedimentation at the scale of the entire Gulf of Lion, we will hereafter use the term "prodelta" for the zone of high sediment accumulation including the delta front and the prodelta.

Apart from the Rhone and Petit Rhone, several secondary rivers (Hérault, Orb, Aude, Agly, Tet and Tech) are located along the western coast of the Gulf of Lion (Fig. 1) and have a torrential regime (Roussiez et al., 2005). On average, they account for slightly more than 5% of the total inputs of particulate matter (0.45 Mt/year) to the Gulf of Lion (Sadaoui et al., 2016). These rivers have experienced, as the Rhone, a drastic decrease of sediment supply to the coast during the last century (Brunel et al., 2014 and references therein).

Sedimentation rates

Sedimentation rates off the Rhone mouth and on the shelf have been studied at event scale (i.e. a few days) and over long time scales (i.e. decades to centuries) using tracers and bathymetric differentials. In the short term and close to the Rhone mouth, sedimentation is very variable from one flood to another, which would not only depend on the river discharge but also on wind and wave conditions (Maillet et al., 2006). For example, a 0.6 m thick deposit was generated at 20 m depth after the 2002 flood characterized by a peak in liquid discharge of more than 9000 $m^3 s^{-1}$, while a deposit of only 0.2 m was generated during the December 2003 flood with similar water discharge.

In the longer term, Sabatier et al. (2006) used bathymetric differentials to highlight several points: (1) the reduction of storage on the Rhone prodelta by a factor of 2.5 to 4 on a time scale of one century; (2) the erosion of prodeltas when they are no longer or insufficiently fed by the rivers which is the case of the Rhone, each time the mouth has been moved naturally or artificially (the last time in 1895). The average storage on the Rhone prodelta between 1895 and 1974 is estimated by Sabatier et al. (2006) at 5 Mt/year. Furthermore, apparent sedimentation rates of 35–48 cm/yr have been estimated on the Rhone prodelta from the $^{137}Cs/^{134}Cs$ ratio (Calmet and Fernandez, 1990; Charmasson et al., 1998). The area characterized by these high sedimentation rates is of restricted dimensions as evidenced by the fact that more than 40% of the ^{137}Cs inventory of a 480km² area in front the Rhone mouth would be concentrated on 30 km² (Charmasson, 2003). Indeed, according to Radakovitch et al. (1999), the maximum accumulation rates decrease rapidly seawards by a factor of 10 over 9 –10 km, and a factor of 100 at 20 km. Moving away from the near-mouth area, the spatial distribution of the sedimentation rates shows a preferential accumulation on the S-SW direction from the Rhone mouth (Fernandez et al., 1991; Durrieu de Madron et al., 2000; Lansard et al., 2007) and a general linear decrease with water depth (Miralles et al., 2005). Sedimentation rates over the shelf are between 0.1 and 0.2 cm/year (Miralles et al., 2005).

Currents and waves

Understanding the spatial and temporal sediment transport dynamics requires an understanding of current and wave forcing. Weather in the Gulf of Lion is dominated by continental winds, namely Mistral and Tramontane, associated with a short fetch and therefore low waves near the coast. Under these conditions, the Rhone plume stretches seaward with a comma shape (Estournel et al., 1997). On the continental shelf, currents form gyres induced by the wind curl with amplitudes of about 0.2 m s^{-1} (Estournel et al., 2003; Petrenko et al., 2008). The currents induced by these prevailing northerly winds are interrupted mainly in autumn and winter by storms blowing from the east or southeast accompanied by swells with significant heights approaching 6 m and periods greater than 10 s at 32 m depth (data from Sète wave buoy https://candhis.cerema.fr). The Rhone plume is then pushed against the coast (Gangloff et al., 2017) and deepens due to downwelling induced by the coastal

blocking (Many et al., 2018). On the shelf, wind-induced currents are strong (>0.5 m s^{-1}) oriented along the isobaths southwestwards (Bourrin et al., 2015; Mikolajczak et al., 2020). These currents strengthen in the southwest due to the shelf narrowing, finally leading to the downwelling of coastal water at the tip of the Gulf into the Cap de Creus Canyon, limited in autumn to 300–400 m depth by stratification (Ulses et al., 2008c; Mikolajczak et al., 2020). This limitation can be exceeded in winter, when the water column near the coast is cooled by heat losses associated with northerly winds. The excess of density gained allows the dense water formed preferentially near the coast, after having flowed over the shelf often with the help of easterly winds, to penetrate deep into the Cap de Creus Canyon. These gravity currents approach 1 m s^{-1} due to the steep bathymetric slopes and the channeling of the flow by the canyon topography. This dense shelf water cascading can reach during the coldest winters, the deep basin around 2000–2500 m depth (Canals et al., 2006; Ulses et al., 2008b; Durrieu de Madron et al., 2013; Palanques and Puig, 2018).

Resuspension and sediment transport

Eastern storms produce resuspension of sedimentary deposits, either by strong currents or by waves. According to Dufois et al. (2008) based on the results of a one-year hydrodynamic simulation, the sandy areas located up to 30 m depth are dominated by strong wave-induced bottom shear stresses allowing sand transport, while sediment accumulation on the middle shelf between 30 and 100 m depth would be explained by a negligible effect of the currents and a decreasing influence of waves, and finally, the outer shelf would be affected by stronger currents allowing erosion of the fine sediment deposits draping relict sands.

Due to the difficulty of instrumenting the continental shelf, there is little experimental evidence of these episodes of intense sediment transport. Nevertheless, altimeter deployments have shown erosion of several centimeters during storms, followed by deposition of equivalent sediment thicknesses, at 28 m water depth, 2 km off the mouth of the Têt River to the southwest of the Gulf of Lion (Guillen et al., 2006; Bourrin et al., 2008). Offshore of the Rhone mouth, at 18 m water depth, Marion et al. (2010) also showed significant sediment dynamics over one winter, with two depositional sequences of 5–6 cm each following moderate floods, and two erosional sequences of about 4 cm during storms. Furthermore, Dufois et al. (2014) observed over 3 months at 21 m water depth northeast of the Rhone River mouth, two erosional episodes of 2 cm each, associated with waves of 3–4 m of significant height. These observations over relatively short periods do not allow for long-term assessments such as sedimentation rate measurements, but they do show that the first centimeters of sediment are subject to frequent physical disturbances during floods and storms. Such short-duration events (typically one day for storms and a few days for floods which most often are coupled with the storms) must be therefore taken fully into account to quantify impacts on the sediments (Durrieu de Madron et al., 2008). Whereas the above observations on sediment dynamics are limited to shallow depths, gliders equipped with optical and acoustic sensors, deployed during storms and following cross-shore transects through the Gulf of Lion shelf, have found increases in suspended matter concentrations as far as the shelf break. Such increases impact the entire water column on the inner and mid-shelf with concentrations of a few tens of mg/L, and are limited to a ~30 m thick bottom nepheloid layer with concentrations of a few mg/L on the outer shelf (Bourrin et al., 2015; Gentil et al., 2022). By integrating the effect of successive storms, this transport could carry particulate matter from the Rhone's vicinity to the southwestern end of the Gulf of Lion (Gentil et al., 2022).

Sediment budget of the Gulf of Lion

From 2003 to 2012, numerous winter mooring deployments in the Cap de Creus Canyon at several hundred meters depth have shown that strong currents, whether related to storms alone or intensified during dense water cascading, were accompanied by typical suspended matter concentrations of 50 mg/L (Puig et al., 2008; Palanques et al., 2008, 2012). Canals et al. (2006) and Puig et al. (2008) claimed that dense shelf water cascading is able to transport large amounts of sediment from the shelf and upper slope to the deep parts of the canyon. 3D models coupling hydrodynamics and sediment transport (Ferré et al., 2008; Ulses et al., 2008a; Dufois et al., 2014) computed net exports from the Gulf of Lion shelf of 6.7 Mt for winter 1998–1999, 10.3 +- 5.8 Mt for winter 2003–2004 and

6.1 Mt for 3 months in autumn-winter 2007–2008. These exports are of the same order of magnitude as the mean Rhone River supplies. However, it has been established (see above) that a large fraction of these river-sourced particulate matter supplies is stored on the river prodelta. On the other hand, external inputs from biology and atmospheric deposition as well as from secondary rivers inputs are much lower than these values: atmospheric inputs represent 0.3+-0.2 Mt/year (Durrieu de Madron et al., 2000); the algal biomass buried in the sediment represents 0.4 Mt/year based on the estimate of organic carbon by Many et al. (2021) multiplied by 3 for total biomass as suggested by Durrieu de Madron et al. (2000); supplies from rivers other than the Rhone represent on average only 5% of total river inputs (Sadaoui et al., 2016). Altogether these values suggest a sediment deficit for the Gulf of Lion continental shelf beyond the Rhone prodelta, which is inconsistent with the accumulation rates provided by geochemical tracers. However, great caution must be exercised due to the uncertainties associated to each term: (1) the export from the shelf derived from modeling over-simplifies complex processes; (2) the accumulation rates are "apparent" as they are based on assumptions such as continuous sedimentation and no post-deposition mobility of sediments (Appleby and Oldfield, 1983; Appleby, 1998); and (3) the disparate time scales associated with each of these estimates in a highly unsteady context (the accumulation rates correspond to durations of the order of a century, whereas the Rhone inflows and exports in the Cap de Creus Canyon concern only the last few years.

Objectives

The present study aims at constraining the sedimentary particle dynamics over the Gulf of Lion shelf and the main export routes towards the continental slope, thus contributing to address the outstanding question of the Gulf of Lion's sediment budget. Our ultimate objective is documenting the spatio-temporal variability of erosion, transport and deposition processes over the various morpho-sedimentary units of the Gulf of Lion in response to two strongly contrasting periods in terms of storminess. Preceding studies focused on shorter periods of time and on a few storm and flood events (Ulses et al., 2008 ; Dufois et al., 2014). Here, the driving idea is to integrate a longer period (i.e. two autumn-winter seasons), embedding highly diversified situations from the meteo-oceanic forcing viewpoint, as expressed by the frequency and intensity of storms, winter heat losses and floods. Such an approach broadens former conceptions of the possible impacts of such events when considered individually, brings in the cumulative effects on a seasonal scale, and allows assessing the system response to two successive seasonal cycles dominated by marked differences in the frequency and intensity of forcings. We consider the spatial variability issuing from these impacts at the scales of the Rhône prodelta —the main current primary depocentre along the shoreline—, and the various morphosedimentary domains of the shelf together with their connection with the continental slope.

2. Material and methods

We use the sediment transport model MUSTANG ((MUd and Sand TrANsport modeling, Le Hir et al., 2011) adapted to sand-mud mixtures forced by the hydrodynamic model SYMPHONIE (Marsaleix et al., 2008, 2019) coupled to the wave generation and propagation model WAVEWATCH III3 (Tolman et al., 2009). The implementation of the combined wave-current interaction parameterization is described in Michaud et al. (2012). The coupling of SYMPHONIE and WAVEWATCH III is described in Mikolajczak et al. (2020) who applied it to the study of the 2010-2011 autumn/winter, marked by several eastern storms. The numerical grid of the circulation model (Fig. 1) covers most of the western Mediterranean Sea using a curvilinear bipolar Arakawa C-grid with 40 generalized sigma levels on the vertical. The bipolar grid allows a horizontal resolution between 300 and 500 m over the entire Gulf of Lion shelf and gradually lowers the resolution towards the south of the domain. This configuration is strictly identical to Mikolajczak et al. (2020). The coupled current-wave hydrodynamic simulation starts on 15 August 2010 and run until 16 April 2012. Time-averaged files (with current, vertical diffusivity, and bottom stress) were created to force the "offline" sediment transport simulation with a maximum frequency of 12 h reduced to 3 h during the strongest storms. The sediment simulation was run from 31 August 2010 to 16 April 2012.

2.1 General principle of the sediment transport model

Sediment dynamics depend on a combination of several processes. Erosion, enabled by sufficiently high bottom shear stresses, is (together with river inputs) the main source of particulate matter to the water column. Subsequently, currents drive the suspended particulate matter (SPM) transport. At the same time, the sedimentation velocities, dependent on the particle's characteristics, limit the residence time of the suspended matter in the water column. Finally, sedimentation leads to the arrangement of particles in the sediment compartment which determines its subsequent erodibility. The representation of these processes is detailed below.

The coupled wave-current model SYMPHONIE + WAVEWATCH III computes bottom shear stresses and provides them to the sediment model MUSTANG. MUSTANG calculates for several particle classes, the erosion flux according to the sediment characteristics and the bottom shear stresses, and sends this flux to SYMPHONIE. This model is equipped with a module calculating advection diffusion (based on the currents and diffusivities from the model itself) and sedimentation of tracers, using the erosion flux as a boundary condition at the base of the water column. At the end of the redistribution of the suspended matter in the water column by the three just mentioned processes, SYMPHONIE transmits to MUSTANG a sedimentation flux. MUSTANG then manages the integration of this material into the sediment layer according to the size of the particles (sand grains are deposited first) and to the sediment volume concentration.

2.2 Particles classes

The approach used here is close to the one by Ulses et al. (2008a). Two classes of sand (fine, 120 µm and medium, 350 µm), two classes of silt (fine, 8.4 µm and coarse, 31.4 µm) and one class of clay (2.4 µm) are considered. Studies of the resuspended fine fractions in the Gulf of Lion (Curran et al., 2007) showed that few of these particles are present in the water column in their primary form, the suspended population being dominated by aggregates. Similarly, Many et al. (2016) reported that fine fractions are present in their primary form at 5–30%, with this proportion increasing from the inner to the outer shelf. Many et al. (2016, 2018) inferred from the high proportion of 20–300 µm flocs in the suspended matter close to the river mouth, a likely increase of the sedimentation velocity by three orders of magnitude (from µm s^{-1} to mm s^{-1}) compared to primary particles composing the aggregates, thereby intensifying the accumulation of fine sediments over the inner shelf. Because of the difficulty to represent flocculation which probably occurs within the river in many cases (Gangloff, 2017) and whose drivers seem very complex (Thill et al., 2001), an empirical approach was chosen as Ulses et al. (2008a) did, by introducing aggregates consisting of clay and fine silt. Upon resuspension, the flux of each of these constituents directed from the sediment to the water column is separated into two fractions, one of them remaining as primary particles $f_{pp(i)}$ and the other passing into aggregates $f_{ag(i)} = 1 - f_{pp(i)}$, where the subscript i represents clay or fine silt. Upon deposition, the aggregates "deflocculate" and return to their primary class. During the suspension phase, it is necessary to trace the amount of clay and fine silt contained in the aggregates to ensure the mass conservation of these two constituents at the time of deposition. This numerical constraint is achieved by splitting the aggregates into two classes whose concentration corresponds respectively to the concentration of fine silt and clay contained in the aggregates.

Sedimentation velocities of sands and of silt and clay primary classes are calculated respectively by the formula of Soulsby (1997) and Stokes. Table 1 summarizes the characteristics of the particle classes inserted into the model. The aggregates sedimentation velocity was subjected to a sensitivity study which resulted in a value of 0.59 mm s^{-1}, which is between the median of the distribution of sedimentation velocities of flocs in the range 250–500 µm (0.28 mm s^{-1}) and of flocs above 500 µm (0.78 mm s^{-1}), measured by holographic camera in the freshwater influenced area off the Rhone River mouth (Many et al., 2019). The sedimentation velocity for coarse silts is close to the median of these large flocs. The sedimentation velocity for fine silts prescribed in the model (0.05 mm s^{-1}) is close to the median of particles between 20 and 125 µm from the latter authors (i.e. 0.07 mm s^{-1}). In practice, it can be stated that these different classes of particles (whatever we name them particles or flocs)

have sedimentation velocities that are close to the most likely values observed by Many et al. (2019) in the different size ranges. The sedimentation velocity of the aggregates is near that of the coarse silts, which can be seen as a step forward towards a representation of the scattering of sedimentation velocities existing in the natural world.

Sediment class	**Diameter (μm)**	**Sedimentation velocity (mm s^{-1})**
medium sand	350	49
fine sand	120	10
coarse silt	31.4	0.75
fine silt	8.4	0.053
clay	2.4	0.0044
aggregate	/	0.592

Table 1. Characteristics of the particle classes introduced in the sediment model. As explained in the text, aggregates appear only in the water column and are redistributed between clays and fine silts when in the sediment.

2.3 Sediment transport model parameterizations

The formulations used are given by Le Hir et al. (2011) for sand and mud mixtures. Since these authors present different formulations, the choices made for each law are specified here. The erosion flux E expressed in kg m^{-2} s^{-1} is given according to the Partheniades-Ariathurai formula initially designed for cohesive sediment which can also represent the pick-up process of fine sands (the bedload transport is not represented):

$$E_{m/s} = E_{0(m/s)}\left(\frac{\tau_b}{\tau_{cr(m/s)}} - 1\right)^{n(m/s)} \text{ if } \tau_b > \tau_{cr(m/s)} \quad (1)$$

E_{0m} and E_{0s} are the erosion fluxes. τ_b is the bottom stress (combined from currents and waves) calculated by the coupled model SYMPHONIE + WAVEWATCH III following Soulsby and Clarke (2005) and τ_{cr} is the critical stress for erosion. Indices m and s refer to cohesive and non-cohesive sediment (respectively mud and sand for ease of simplicity). As in Le Hir et al. (2011), three cases are considered depending on the fraction of clay and silt in the surface sediment. Below a fraction fr_1 (between 0 and 1), the sediment is considered non-cohesive, and the critical stress $\tau_{cr(s)}$ is calculated after the Shields diagram from the mean sand diameter d_s. Above a fraction fr_2, the sediment is considered cohesive and the critical erosion stress $\tau_{cr(m)}$ is fixed. At the transition between fr_1 and fr_2, the parameters involved in the erosion flux, E_0, τ_{cr} and n are interpolated between their values calculated in the cohesive and non-cohesive regimes from an exponential function as proposed by Mengual et al. (2017).

fr_1 depends on the mean sand diameter following:

$$fr_1 = \alpha d_s \quad (2)$$

where α is a constant and d_s is expressed in m.
The erosion flux of the different classes of sand and mud is then proportional to the mass fraction of this class in the surficial sediment.

During the deposition phase, sediment layer management is performed as in Le Hir et al. (2011). Pores between coarser particles are first filled up with finer particles before increasing the layer thickness or adding a new layer. The deposition flux D is calculated with the Krone formula assuming an infinite critical deposition stress which results in:

$$D = w_s C \quad (3)$$

where w_s is the sedimentation velocity. C is the mean concentration of the first layer above the bottom for fine particles, while for sand classes, to account for the rapid increase in concentration near the bottom, as in Le Hir et al. (2011), C is calculated at a reference level (here set at 2 cm above the bottom after calibration tests) using the Rouse profile, which depends on the sedimentation velocity and bottom stress. The Rouse profile is then normalized to be consistent with the average concentration over the first layer. Deposition is prevented in the riverine part of the Rhone River, poorly represented by the model grid. Consolidation is not taken into account in our configuration.

The values of the parameters of the different parameterizations are given in Table 2. These values were chosen from a number of simulations performed with different parameter sets and from comparisons of results with available observations of suspended matter concentration.

Parameter	Value	Unit
$E_{O(m)}$	10^{-5}	kg m^{-2} s^{-1}
$E_{O(s)}$	5.10^{-4}	kg m^{-2} s^{-1}
$\tau_{cr(m)}$	0.1	N m^{-2}
$n_{(m)}$, $n_{(s)}$	1	-
fr_2	0.7	-
α	1000	m^{-1}
$f_{pp(clay)}$	0.25	-
$f_{pp(finesilt)}$	0.25	-

Table 2. Values of the sediment model parameters used in the simulation

The critical stress for erosion τ_{cr} is of the same order of magnitude as the value of 0.2 N m^{-2} used by Ulses et al. (2008a) for the same site, which is a typical value for most coastal and estuarine areas (Dyer, 1986). As noted by Ulses et al. (2008a) a large interval of values of the mud erosion flux is found in the literature ($6.25\ 10^{-6}$ –$2\ 10^{-3}$ kg m^{-2} s^{-1}). Our value is of the same order of magnitude than the value of $3\ 10^{-5}$ kg m^{-2} s^{-1} found in Ulses et al. (2008a). Similarly for the sand erosion flux which is close to the $2\ 10^{-4}$ value used by Ulses et al. (2008a) and Le Hir et al. (2011). We recall that a sensitivity study to the value of these parameters can be found in Ulses et al. (2008) for the Gulf of Lion. α is in the range 1–3 10^3 m^{-1} suggested by Le Hir et al. (2011). The values of fr_2 and $n_{(m)}$ were also suggested by Le Hir et al. (2011). The value of $f_{pp(i)}$ is based on calibration tests and the studies of Durrieu de Madron et al (2005) and Ulses et al (2008a).

2.4 Sediment initial state

As in Ulses et al. (2008a), the initial grain size distribution in the sediment was specified for the 5 sediment classes of Table 1 by interpolating the sediment grain size inferred from 787 cores collected over the whole Gulf of Lion (S. Charmasson, V. Roussiez, A. Grémare, N. Frumholtz, S. Berné, pers. comm.). Two interpolations were performed: a first classical one depending on the distance and a second one depending on a "bathymetric distance" i.e., the depth difference between the observation and the relevant grid point. These two estimates were further combined. In order to represent a general tendency for the average sediment diameter to increase towards the coast and to avoid particularities of certain data that could strongly impact the results, we favored bathymetric

interpolation over the entire shelf except for the area near the mouth of the Rhone River for which the distance to the data is favored. Once the fractions are defined at each grid point, the mass concentrations of each class are then calculated following Mengual et al. (2017) by multiplying the fractions by the sediment bulk density C_{bulk} determined following:

$$C_{bulk} = \frac{C_{relmud}}{1 + f_s \cdot \left(\frac{C_{relmud}}{\rho_s} - 1\right)} \quad (4)$$

where C_{relmud} is the relative mud concentration set at 500 kg m^{-3}. f_s is the total sand fraction and ρ_s is the grain density equal to 2600 kg m^{-3}. Since for elevated sand fractions, C_{relmud} is not realistic, in these cases, C_{bulk} is constrained not to exceed 1742 kg m^{-3}, which corresponds to highly mixed sediment density (Mengual et al., 2017).

The mass concentrations are then assigned to the 100 layers of sediment of thickness 0.5 mm. After this first initialization phase, a spin-up of 6 months (the first 6 months of the final simulation including one autumn and winter period) is performed. The "true" simulation is then reinitialized by setting the concentrations of the 100 layers to the average concentrations obtained on the first 3 mm of the surface sediment at the end of the spin-up. The concentration of the different classes is shown in Figure 2. Outside the area off the Rhone River mouth, sands are the dominant fraction up to a water depth ranging between 20 and 40 m. Beyond this proximal area, coarse silts become predominant between 40 and 60 m depth, followed by the finest particles, fine silts and clays. On the outer shelf and particularly on the shelf break, the sandy fraction increases again, by the presence of relict sands mixed with mud. High sand contents occur in the upper reaches of the Cap de Creus Canyon, on its southern flank and downstream of it. Off the secondary rivers, the deposition of silts occurs very close to the mouth, thus breaking the dominance of sand at the shallowest depths. South of the Rhone River mouth, fine sediments are deposited further offshore. These results are consistent with analyses of the fine sediment fraction in the Gulf of Lion by Aloisi et al. (1979) reproduced in Roussiez et al. (2005), showing that: (i) the maximum of fine particle contents in front of the Aude River mouth is located at a shallower depth than off the Rhone River mouth, (ii) outside the river mouths, the fine particle contents increase from the coast down to 50 m depth, which corresponds approximately to the limit of the swell influence (Roussiez et al., 2005) and to the location of the mid-shelf mud belt.

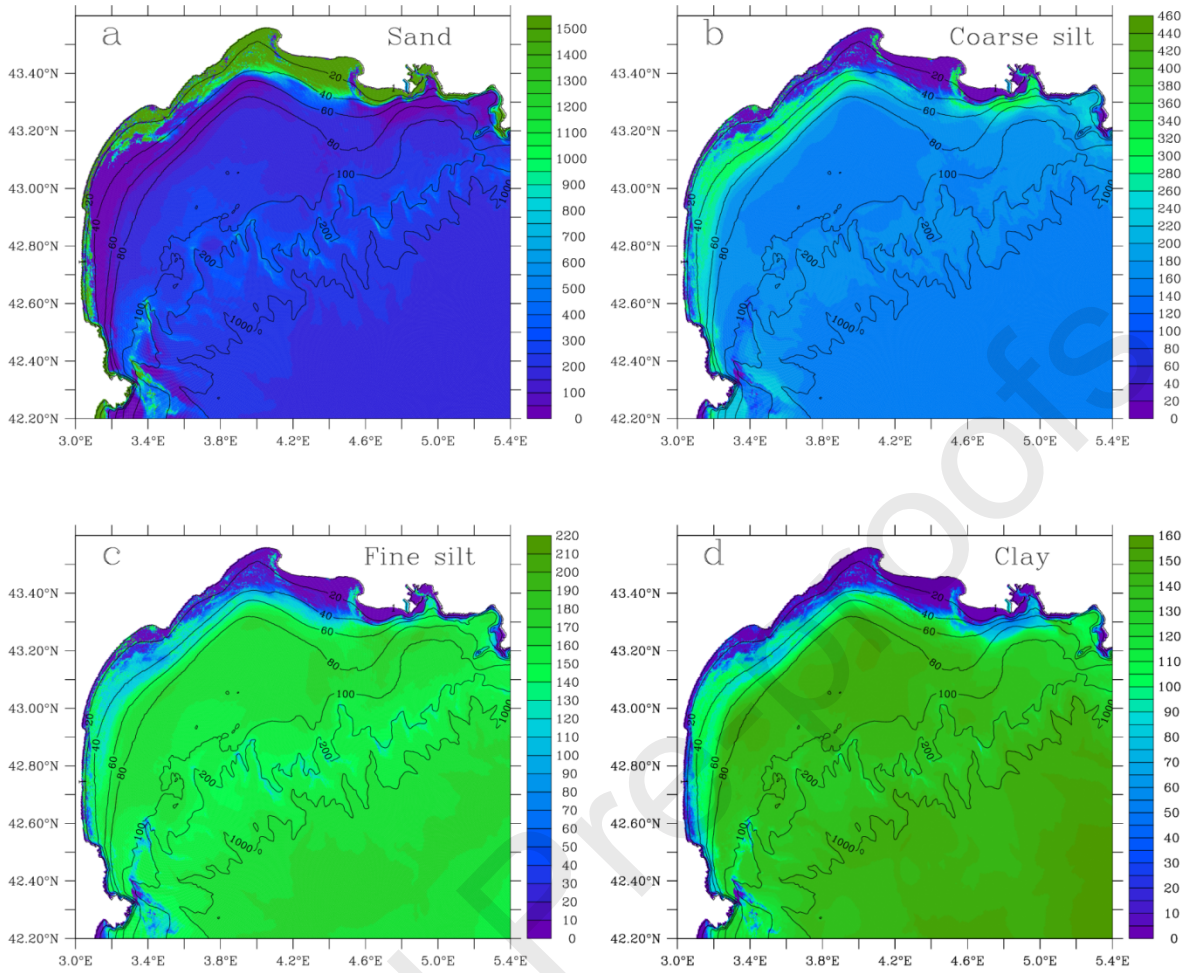

Figure 2. Concentration (kg m^{-3}) of the granulometric fractions in the model initial state: (a): sand (fine + medium), (b): coarse silt, (c): fine silt, (d): clay. Note the scale varies in the different subfigures.

2.5 Simulation forcing

The forcing (lateral boundary conditions, air/sea interface, tides, river discharges) for the hydrodynamic simulation are identical to those described in Mikolajczak et al. (2020) where details can be found. SPM concentrations in rivers are derived from daily observations for the Rhone River and empirical formulas for the secondary rivers. For the Rhone River, the database of the Rhone Sediment Observatory (Thollet et al., 2021) provides the suspended matter at Arles (Arles/CMES-2 product). For the other rivers, the relationship between SPM concentration and water discharge is from Sadaoui et al. (2016). SPM concentrations are then partitioned into sand, silt, and clay following the relationships of Antonelli et al. (2008) for the Rhone River, which depend on total SPM (sand/silt concentration increasing/decreasing with SPM concentration and sand content varying between 5% and 20%). Silts are then split 64%: 36% between coarse and fine fractions. The fine silts and clays are distributed between primary particles and aggregates with the same percentages f_{pp} as the erosion fluxes (Table 2). The inputs of particulate matter from the atmosphere and at the open boundaries are neglected.

2.6 Observations

Wave data from Espiguette wave buoy (https://candhis.cerema.fr) are used to evaluate the WAVEWATCH III model.

As explained below, since the evaluation of the hydrodynamic simulation for winter of 2010-2011 was already performed by Mikolajczak et al. (2020), we focus here mainly on the second winter (i.e. 2011-2012) of our study period and on the current at 300 m in the Cap de Creus Canyon, the only time series we have over several months for the two years. For winter 2011-2012, we make use of the temperature time series measured at the POEM buoy located at 28 m depth southwest of the Gulf of Lion and of the near-bottom temperature and current time series at 1000 m depth in the Cap de Creus Canyon (see Fig. 1 for the position of the points). These time series are presented in Durrieu de Madron et al. (2013).

Regarding the evaluation of the sediment model, we use the SPM concentration determined both at the POEM buoy and from a glider that carried out several transects between the POEM buoy and the 100 m isobath approximately at the same latitude, in March 2011 during the CASCADE campaign. These data presented in Bourrin et al. (2015), illustrate the impact of a strong storm. A SPM time series also exists for the Cap de Creus Canyon head at 300 m depth, 6 m above the bottom, during the winters of 2011 and 2012. These observations are presented in Martin et al. (2013) for winter 2011 and in Palanques and Puig (2018) for winter 2012.

3. Meteorology and sea state

Figure 3 illustrates the simulation period with the significant wave height measured at a depth of 32 m near Espiguette (Fig.1) and simulated by WAVEWATCH III at the same point, the bottom stress and heat flux averaged over the coastal strip (depth less than 50 m) of the Gulf of Lion shelf, the river discharges distinguishing the Rhone from the sum of secondary rivers. The two autumns of 2010 and 2011 were punctuated by marine storm periods identified by significant wave height and bottom stress peaks (Fig. 3 a-b). However, one can notice that in autumn 2011, marine storm events were more intense (Hs > 3 m, bottom shear stress> 2 N m^{-2}) than in autumn 2010 and followed one another over a period of a few weeks, at the end of October/early November. Regarding the two winter periods, a striking difference appears between the two winters. From January to March 2011, several stormy periods followed one after another, including the March 2011 storm (Fig. 3a) documented by the CASCADE campaign (Martín et al., 2013; Bourrin et al., 2015) on which we focus for the validation of the sediment transport model. On the contrary, the winter of 2011-2012 was much calmer in terms of storminess. Considering heat loss, the second part of the first winter (2010–2011) showed short periods of heat losses (Fig. 3c), unfavorable conditions for dense water formation. During the second winter, from November 2011 to the end of February 2012, heat losses were permanent, in particular with a long-lasting episode with high values in February. These results are in agreement with the meteorological analysis of eight winters presented by Mikolajczak et al. (2020). The severity of winter 2012 caused an exceptional episode of coastal dense water cascading in the western canyons as documented by Durrieu de Madron et al., (2013) and Palanques and Puig, (2018). The previous comparable event was 6 years before.

The Rhone discharge increased in autumn and winter though within moderate levels apart from the flood of early November 2011 (Fig. 3d). The secondary rivers almost always had a very low discharge except for a few episodes and in particular in March 2011, during the CASCADE campaign, when they exceeded the Rhone discharge.

In summary, the strongest marine storms of the entire simulation period occurred in October 2010, March 2011 and late October / early November 2011. Freshwater discharge peaked at the end of this last event, with the Rhone reaching the highest discharge of the entire study period. The main flood of rivers on the west coast took place in March 2011. The winter 2012 was exceptionally cold with cascades of dense coastal water over the continental slope.

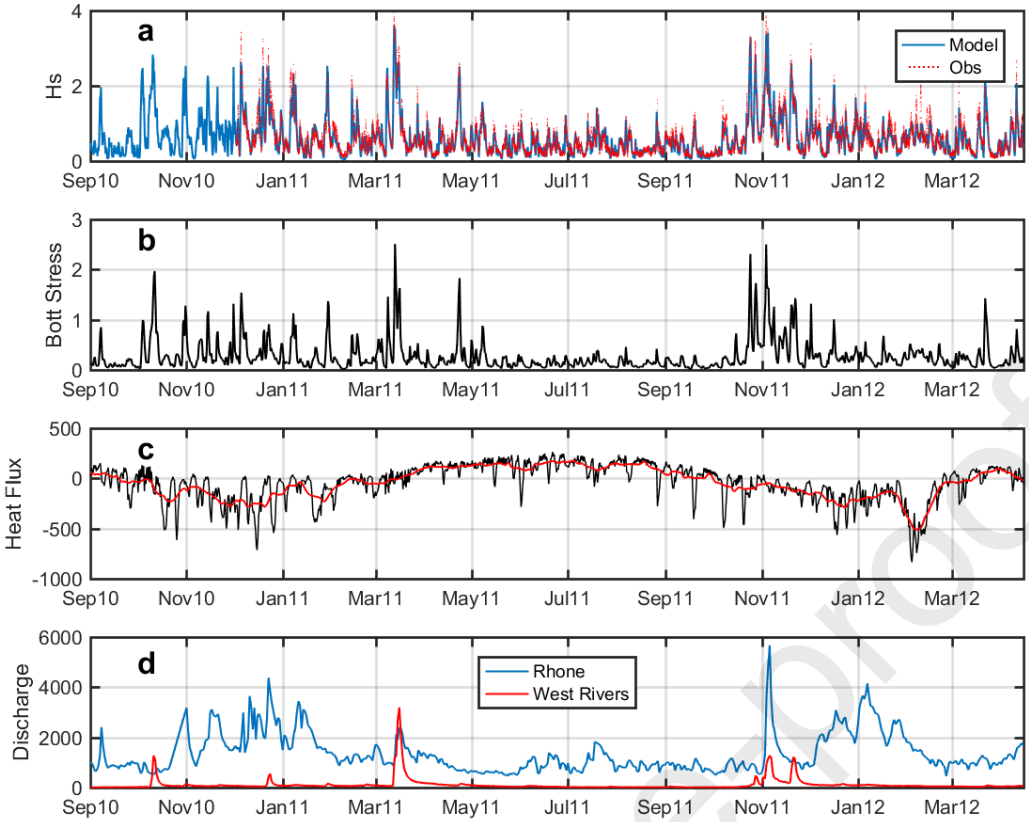

Figure 3. (a): significant wave height Hs (m) measured (red dots) and simulated (blue line) near Espiguette, (b): bottom shear stress (N m^{-2}) averaged over the 0–50 m depth belt, (c): heat flux (W m^{-2}) averaged over the 0–50 m depth belt (in black, and moving average in red), and (d): river discharge (m^3 s^{-1}) in blue: the Rhone River, in red: the sum of the rivers discharging on the west coast of the Gulf of Lion.

4. Assessment of the simulation

4.1 Hydrodynamic simulation

The first part of the simulation (autumn-winter 2010–2011) was evaluated against hydrological and current observations on the shelf and in the Cap de Creus Canyon (Mikolajczak et al., 2020). The latter authors emphasized the intensification of currents during storm events causing preferentially alongshore export towards the North Catalan shelf (south of the Cap de Creus). The rare events of dense water formation followed by shallow cascading triggered by eastern storms caused little export of water from the shelf below 200 m depth. This simulation has been extended to 2012 for this study. In Fig. 4 we compare the measured and simulated temperatures on the shelf at the POEM buoy station and in the Cap de Creus Canyon axis at 1000 m depth (see Fig. 1). These results attest to a cold winter with water temperatures below 10°C on the shelf. The currents close to 1 m s^{-1} at 1000 m depth and oriented down-canyon, along with temperatures below 12ºC indicate the deep cascading of the dense coastal waters into the canyon (Durrieu de Madron et al., 2013). Both on the shelf and in the canyon, the model generally reproduces the seasonal timing of temperature with the peak of cooling triggering cascading in early February, and the warming and cessation of cascading in mid-March in the observations, and late March in the model. The intensity of cooling and cascading currents in the canyon is reproduced by the model.

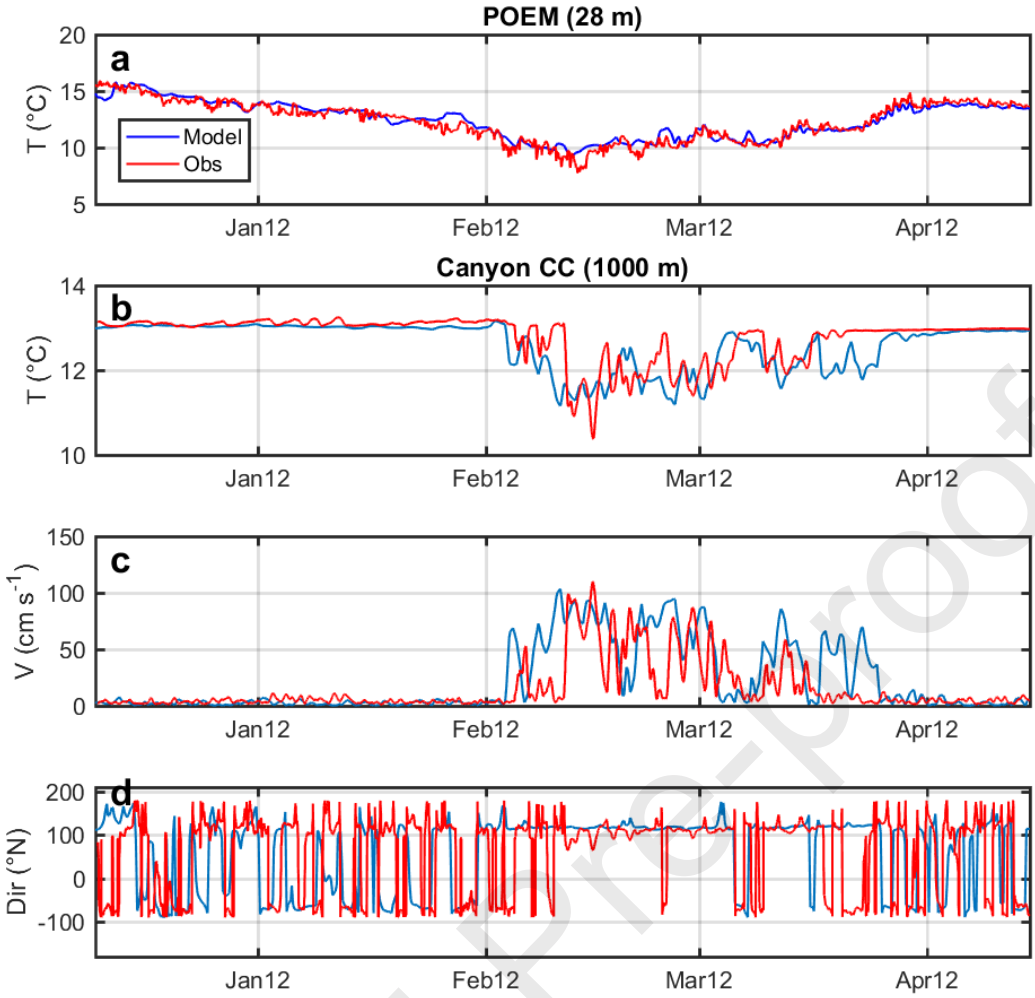

Figure 4. (a): observed (red) and simulated (blue) temperature at the POEM buoy station. (b): same for bottom temperature at 1000 m depth in the Cap de Creus Canyon. (c and d): same as previous for the bottom current velocity and its direction (see locations in Fig. 1).

4.2 Sediment transport simulation

The CASCADE campaign (March 2011) gathered valuable observations of the SPM on the Gulf of Lion shelf during a storm and a flood. The comparison of the model with these observations is the first point of this section. The second point concerns the observation of the particulate matter export through the upper reach of the Cap de Creus Canyon at 300 m of water depth which is available for each modeled winter.

4.2.1 Storm and flood of March 2011

The stormy March 2011 was marked by three days of swell on the 8th, the 12th (the highest) and the 15th. Heavy rains also fell over the western Gulf of Lion which led to flooding of the secondary rivers. Floods started on March 13th and peaked on March 16th - 17th. The Rhone River, to the east, was barely affected. Observations collected during the period are described in detail in Martin et al. (2013) and Bourrin et al. (2015).

Figure 5 shows the impact of these events on the SPM concentration at the POEM buoy station at 1 m below the surface (Fig. 5a) and successive transects across the shelf by a glider (Fig. 5b) and from the model (Fig. 5c). Figure 6 shows at the full scale of the Gulf of Lion on March 19, 2011, the SPM concentration map derived from the first cloud-free MODIS-AQUA satellite image and the corresponding model output.

The events marking the observed time series at the POEM buoy station (Fig. 5a) are generally well

reproduced by the model (in advance for the main peak) as well as the time constants of concentration rise and fall around the main peaks. The difference in timing during the flood period (which is on the order of half a day) and in magnitude of peaks very likely relate to the use of daily averaged discharges and empirical relationships for the solid discharge of the secondary rivers. The model errors (bias and Root Mean Square Error) are -1.4 and 6.0 mg/L respectively, over the observation period.

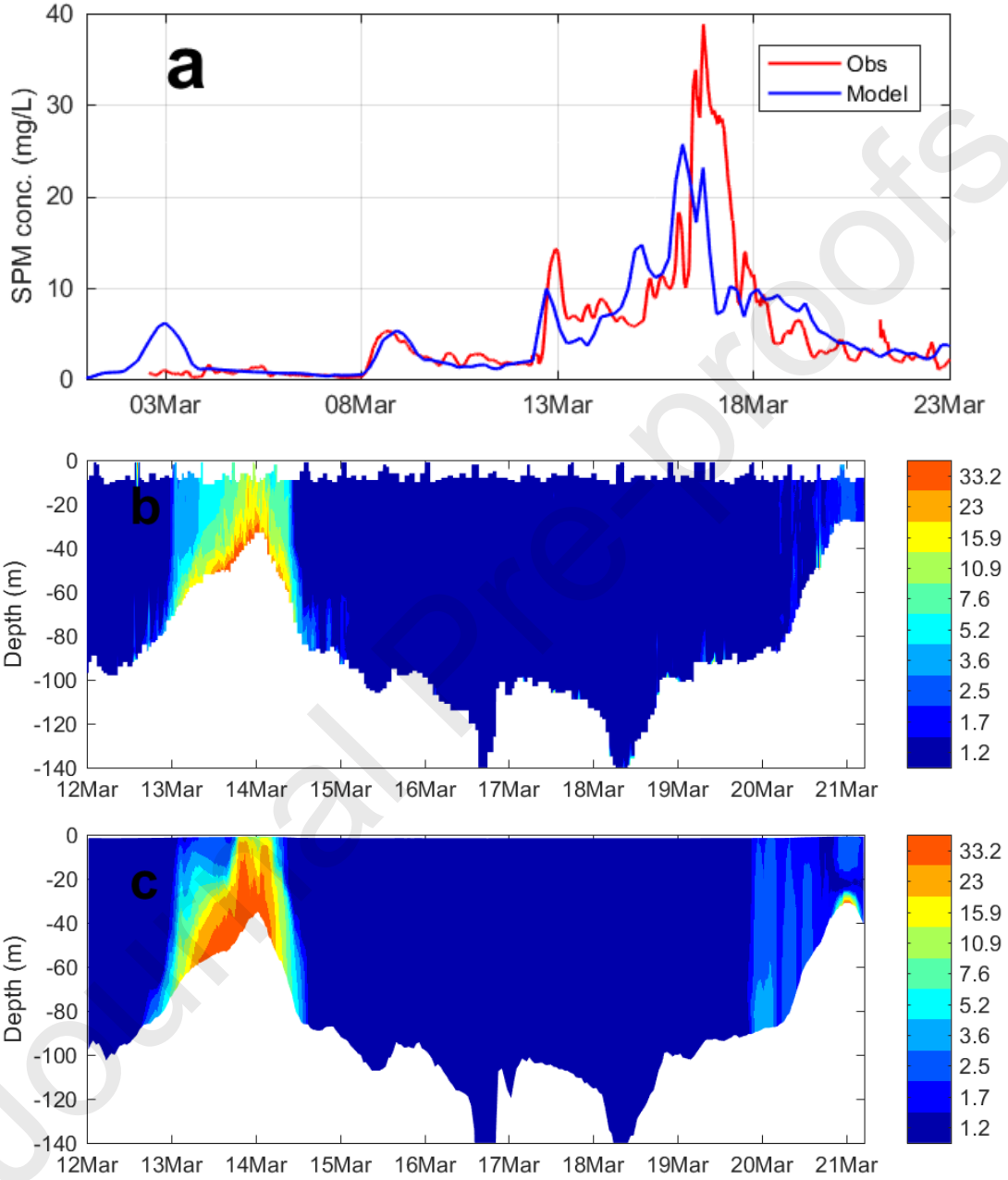

Figure 5. Suspended matter concentration (mg/L) during the CASCADE campaign in March 2011, (a): at 1 m under the surface at the POEM buoy station: observed (red) and simulated (blue) (b): observed along the glider path, (c): simulated along the glider path. The glider moved from the 40 m isobath on March 14 to the shelf break and back toward the coast on March 21 (see rough topography in white). The scale of b and c is logarithmic.

Following the swell peak of the night of 12–13 March, the glider (Fig. 5b) encountered high SPM concentrations between the coast and 80 m depth until the surface but which were maximum at the bottom. At the time of the flood peak of March 17, the glider was on the outer shelf where no signal of the flood was detected. When the glider returned to the coast on March 21, the concentration increased again at depths less than 60 meters though it was only about 2 mg/L. The simulation generally reproduces this behavior with a bias and RMSE of 2.0 and 5.4 mg/L at 30 m depth.

The satellite image of March 19 (Fig. 6a), two days after the flood peak of the western rivers, shows that the entire coastal strip of the Gulf of Lion extending southwards of Cap de Creus coastal promontory, was characterized by surface SPM concentrations of about 5 mg/L. To the northeast, the influence of the Rhone River is recognised by means of a turbid plume directed to the southwest. To the west, in front of the flooding rivers (Hérault, Aude, Orb) the concentration was high over an area extending beyond the 80 m isobath. The model (Fig. 6b) underestimates the concentration of suspended matter to the north in the area under the influence of the Rhone River, and reproduces better the satellite values to the west (underestimation is about 2 mg/L).

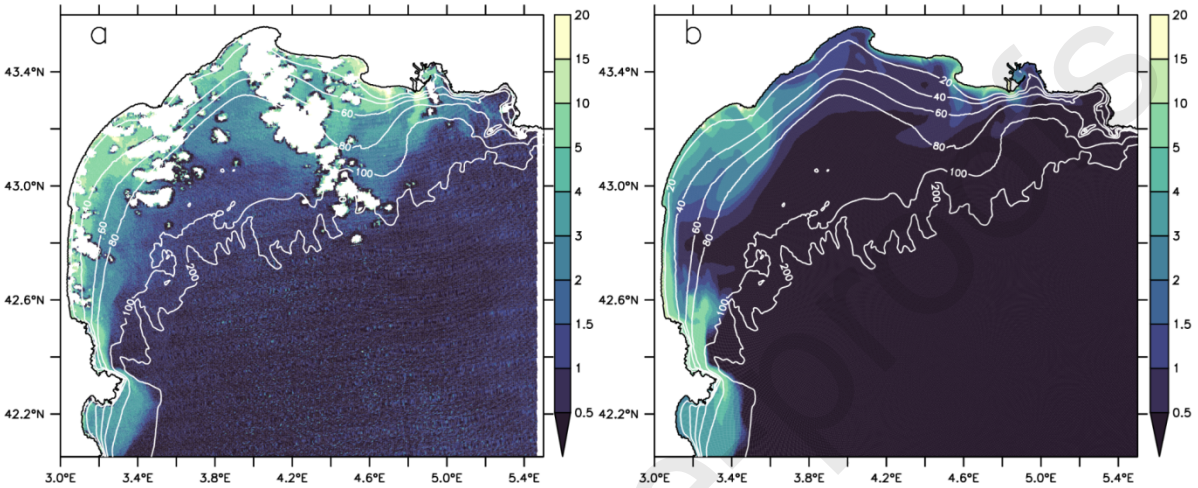

Figure 6. Suspended matter concentration (mg/L) for 19 March 2011. (a): MODIS-AQUA satellite product (Ody et al., 2016) and (b): simulation (surface concentration)

4.2.2 Particulate export into the Cap de Creus Canyon head

Particulate matter concentration and current time series at 300 m in the Cap de Creus Canyon head are shown in Fig. 7. In order to meaningfully compare to the observations, the concentration for each particle class, representing an average over the first layer of the model above the seafloor (whose total thickness is 20 m at the point considered), was reduced to 6 m, i.e. down to the observation level, using the Rouse formula that depends on the sedimentation velocity and bottom turbulence. The simulation shows events of suspended matter concentration peak (Fig. 7a) that are well-phased with the observations and have correct orders of magnitude (bias and RMSE are -0.4 and 1.2 mg/L respectively). The total current (Fig. 7b) as well as the down-canyon component (Fig. 7c) are low out of the 2 winters, in both observations and simulation. During the first winter, the observed current with intermittent peaks is overestimated in January/February and underestimated in March by the model. During the second winter, the strong currents that prevailed for about 2 months as at 1000 m (Fig. 4c) are on average well reproduced although underestimated. In order to evaluate the ability of the model to quantitatively represent sediment export, the cumulative down-canyon sediment flux at the observation point (i.e. product of concentration by down-canyon current) is compared for the 2 periods (Fig. 7d). Even if there is some chronological mismatch in the model, the export cumulated over each season is in the order of magnitude of the observation with an error of +47% and -23% for the two periods, respectively.

It is to be noted that the storm in October 2010, with four days of southeast wind and a significant wave height approaching 4 m west of the Gulf of Lion, was unfortunately not included in the observation period. Following Mikolajczak et al. (2020), it induced, for coastal waters, the shortest residence time of the whole autumn - winter period on the Gulf of Lion shelf. At 300 m, the model indicates a clear increase in the concentration of suspended matter though associated with a weak current, thus not inducing a significant export. It seems that the influence of downwelling hardly reaches 300m depth during this storm, probably because of the early autumn strong stratification. During the CASCADE period in March 2011, also shown in Figures 5 and 6, the suspended matter concentration is underestimated on the shelf. Mikolajczak et al (2020) showed that for this period, the

simulation underestimates the current on the shelf. This underestimation is likely the cause of a too weak resuspension especially on the outer shelf (as Figure 6 suggests) which would impact the concentration passing over the canyon head. On the other hand, the satisfactory comparison with the satellite image (Figure 6) showing the core of the turbid plume bordering the Cap de Creus promontory suggests that the southward export along the coast could be correctly reproduced. After the March 2011 event, the model indicates that the canyon was not fed until autumn 2011, with a first low amplitude event in November 2011. After a few events in December and January, a major export episode was observed and simulated in February 2012 which opened to smaller but incessant peaks throughout March 2012 corresponding to the dense shelf water cascading seen in Figures 4b and c.

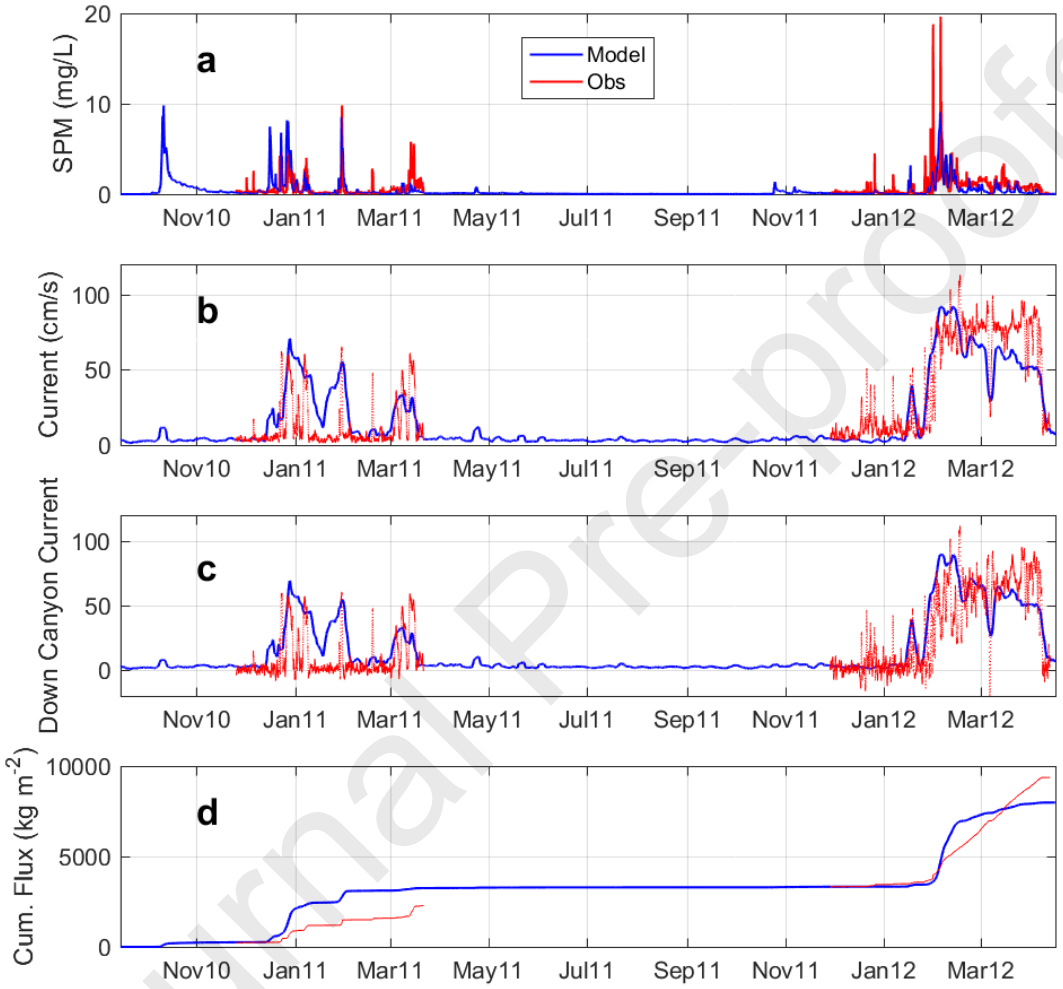

Figure 7. (a): Suspended matter concentration (mg/L) at 300 m in the upper Cap de Creus Canyon, (b) current at the same point, (c): down canyon component of the current, (d) suspended matter cumulative lateral flux. blue: simulation, red: observation (note that the time series of observations is on the one hand shorter than the numerical series and on the other hand discontinuous, which led to the red curve of Fig. 7d being shifted to the blue curve at 2 dates (the December 2010 and 2011) to facilitate the comparison of the model with the observations).

5. Results and discussion

In this section, the sediment dynamics is analyzed from both a spatial and temporal point of view. We consider the specificities related to the area near the Rhone River mouth, to the shelf partitioned according to its different morpho-sedimentary units and to the continental slope. The simulated period is divided into two sub-periods characterized by contrasting drivers of the sediment dynamics: recurrent storms during the first period (2010-2011), floods and dense shelf water formation and cascading during the second period (2011-2012).

5.1 Sediment accumulation in the vicinity of the Rhone River mouth

The change in sediment level in the vicinity of the Rhone River mouth at the end of the simulation (16 April 2012) compared to the initial state (31 August 2010) is shown in Figure 8. It can be associated with two years, as two active seasons (October to March see Figs. 3 and 7) from the sedimentary viewpoint have been simulated.

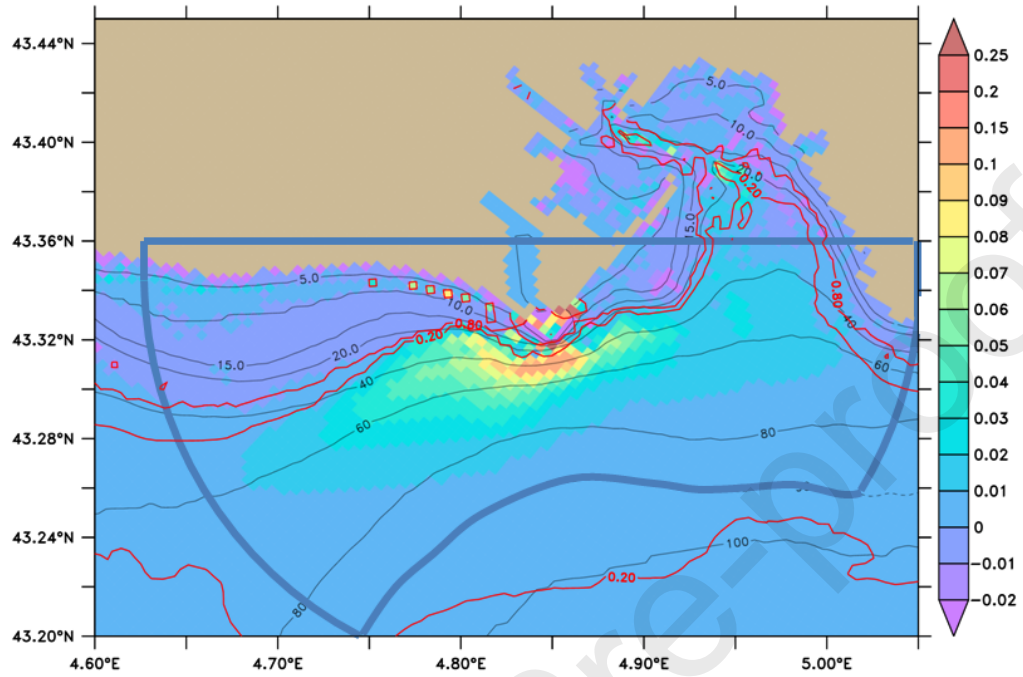

Figure 8. Background color: thickness of deposition (positive) or erosion (negative) in meters resulting from the simulation (between August 31, 2010 and April 16, 2012) in the vicinity of the Rhone mouth. Note the change in color spacing at 0.1 m and the asymmetry of the range of values on either side of 0 (only the purple color corresponds to erosion). Isobaths (m) are in black. The red contours set at 0.2 and 0.8 indicate the sand fraction in the upper first centimeter of the sediment. The thick blue line delineates the box used to calculate the sediment budget (cf. Fig. 9), its offshore limit being the 90 m isobath.

The oblong shape of the prodelta aligned with the isobaths from southwest to northeast is clearly depicted in Figure 8, which also shows an extension of the deposition along the Gulf of Fos channel (north of 43.36 °N) at depths shallower than ~ 20 m. In front of the river mouth, the deposit is well organized from about 30 m depth (note the steepness of the prodelta topography in front of the mouth), with an area of 1.5 km^2 around 30-50 m water depth where the deposit is thicker than 10 cm, decreasing seaward to 1-2 cm at 80 m depth, 3 km further offshore. This deposition is lower but of the same order of magnitude than the one found by Fanget et al. (2013) after the analysis of a sediment core taken at 79 m depth south of the Rhone mouth, which shows an average accumulation of 2.3 cm/year over 45 years from 1963 to 2008.

At about 20 m depth, a sharp transition occurs from a sand-dominated coastal strip adjacent to the shoreline to a mud-dominated belt seawards. Note that deposits exceeding 25 cm appear in some grid points between 10 and 20 m depth. Such deposits appear and disappear during the course of the simulation as a result of floods and storms. Although the resolution of the grid is insufficient to represent this narrow bathymetric band accurately, these processes could reflect that this is a temporary accumulation area (likely lasting a few months).

Finally, a few points located at shallow depths (~<5 m) in front of, and on either side of the Rhone mouth, and particularly to the east, display the thickest deposits (>30 cm), which are composed mostly of fine sand (not shown). These nearshore deposits represent 0.3 Mt which is close to the integrated fine sand Rhone input over the period (0.27 Mt) and may also include redistributions of pre-existing sand. Even if the resolution of the model and the absence of bedload transport prevent us to

claim to correctly represent the sediment dynamics processes within the first 10 m water depth, such a large littoral deposition to the east of the river mouth is consistent with the results of the high-resolution sediment transport modeling over the Rhone delta by Boudet et al. (2017).

The sequence of particulate input from the Rhone River, and of deposition around its mouth is illustrated in Figure 9. Here we consider the region located within an arbitrary distance of 18 km from the river mouth with a northern limit at latitude 43.36°N, and a depth limit set at 90 m (as shown in Fig. 8). This area will hereafter be called the "extended Rhône prodelta". The main phases of deposition are linked to the river discharge events, starting by a moderate discharge period from November 2010 to February 2011, followed by a calm period until November 2011 punctuated by a major flood in terms of solid load, finalized with a pronounced increase peaking by the beginning of January 2012.

The fraction of the SPM discharge deposited over the area under consideration, changes from one period or event to another. Apart from storm periods, 55% to 75% of the material brought by the Rhone are accumulated in the prodeltaic sedimentary deposit. When integrated over the whole period, this percentage drops to 56% (representing 2.3 Mt) due to erosion / export during storms. Conversely, the highest relative accumulation (>80% of the river discharge) occurs during the very calm summer period. However the amounts brought by the river during the summer low water discharge period are minor and have little impact on the total sediment budget. Moreover, phases of decreasing sediment accumulation are rare and their intensity is low, which suggests a massive long-term storage. In conclusion, the proximal region off the Rhone River mouth accumulates sediment even if redistribution occurs at the occasion of particular events as illustrated by the stock variations uncorrelated to the Rhone discharge during the storms of March 2011 and November 2011 (just before the flood occurs for this last event).

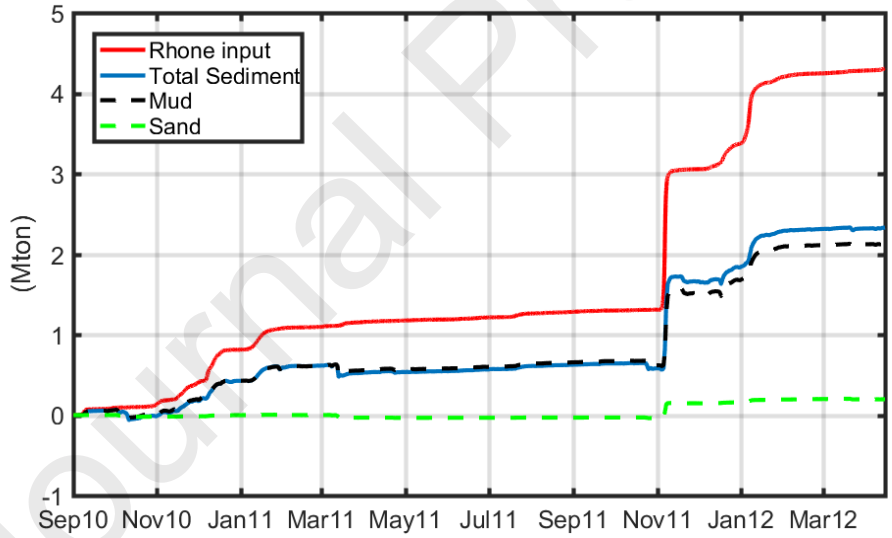

Figure 9. Rhone particulate matter supplies (red) and deposition integrated over the sediment budget area indicated on Fig. 8 (blue). Black and green dashed lines represent the amount of mud and sand in these deposits. Values have been accumulated since the start of the simulation (31 August 2010).

5.2 Spatial and temporal variability of sediment dynamics over the continental shelf

The amounts of deposited or eroded sediment for both years, computed between September 15 and April 15, (encompassing the active season in terms of riverine inputs and storm events) are displayed in Figure 10. The Rhone extended prodelta discussed in the previous section stored sediment during both years, and it is the only place on the shelf storing more in the second year than in the first one due to the November 2011 and January 2012 flood events together with the low storm activity. Another common feature of both years concerns the headlands formed by the Beauduc and Espiguette spits with new deposits around 10-15 m water depth reaching 10 cm in thickness each year (Fig. 10). These deposition areas are consistent with the observations of Sabatier et al. (2006)

who emphasized that these are, along with the Rhone prodelta, the only ones on the coastline between 4 and 5°E to undergo sediment accumulation over the last century. No prodeltaic accumulation is simulated in front of the Petit Rhône in accordance with the results of the latter authors who noticed erosion of an ancient prodelta.

Apart from these two areas, the two investigated years are extremely contrasted: 2011-2012 is associated with very little deposition and erosion (with the exception of the southwestern end of the continental shelf, south of 42.6°N which is discussed in the next paragraph). In contrast, during 2010-2011, the area within the shallower 50 m (more precisely 60 m to the north and 40 m to the west) was reworked, generally with erosional places interspersed with more or less temporary deposition. Beyond this more energetic shallow belt, deposition feeds a mud belt according to the definition of sedimentary units made from granulometric characteristics by Durrieu de Madron et al. (2000). Deposition intensifies from north to southwest and also shifts to shallower depths southward: aligned on the 60 m and 40 m isobaths north and south of 43°N respectively. These depths also are in agreement with the mapping of fine muddy sediment by Aloisi et al. (1973) later repeated by Roussiez et al. (2005). At the mud belt, the order of magnitude of deposition ranges from 1 to 6 mm for the 7 months under consideration. Integrated over the 19 months of simulation, these values change little due to low deposition during the second year, which leads to an "average" sedimentation rate varying spatially from 0.6 to 4 mm/year which could be compared to the 1 to 2 mm/year range obtained over the long term (Miralles et al., 2005).

At the southern tip of the mud belt, a depocenter occupies the bay right north of the Cap de Creus promontory (latitude ~ 42.4°N) where a 2 cm thickness is reached between 40 and 80 m depth in the first year. Although this area, and more generally the south-western end of the continental shelf are heavily reworked in the second year, a net accumulation is obtained over the two years in most of the area. This is in line with the results of De Geest et al. (2008) from ^{210}Pb . In contrast, erosion prevails between the Cap de Creus promontory and Lacaze Duthiers Canyon around the 100 m isobath, and more generally, the shelf break and uppermost slope (200 m isobath) over almost the entire Gulf of Lion (Fig. 10a).

The highly contrasted sediment dynamics of the two periods is driven by contrasting currents and sea states. The storms of 2010-2011 limit the deposition of particulate matter brought by the rivers, and produce resuspension that favors the movement of sediment both from the inner shelf to the mid-shelf and from the northeast to the southwest shelf. The 2011-2012 period, atypical given the low number of storms and the large dense shelf water formation, is opposite. Dense water formation is known to produce gravity currents (Canals et al., 2006) but these are proportional to the bathymetric slope which explains their low intensity on the shelf and therefore their low impact on the sediments. The exception is the southwestern end of the shelf, where the isobaths tighten.

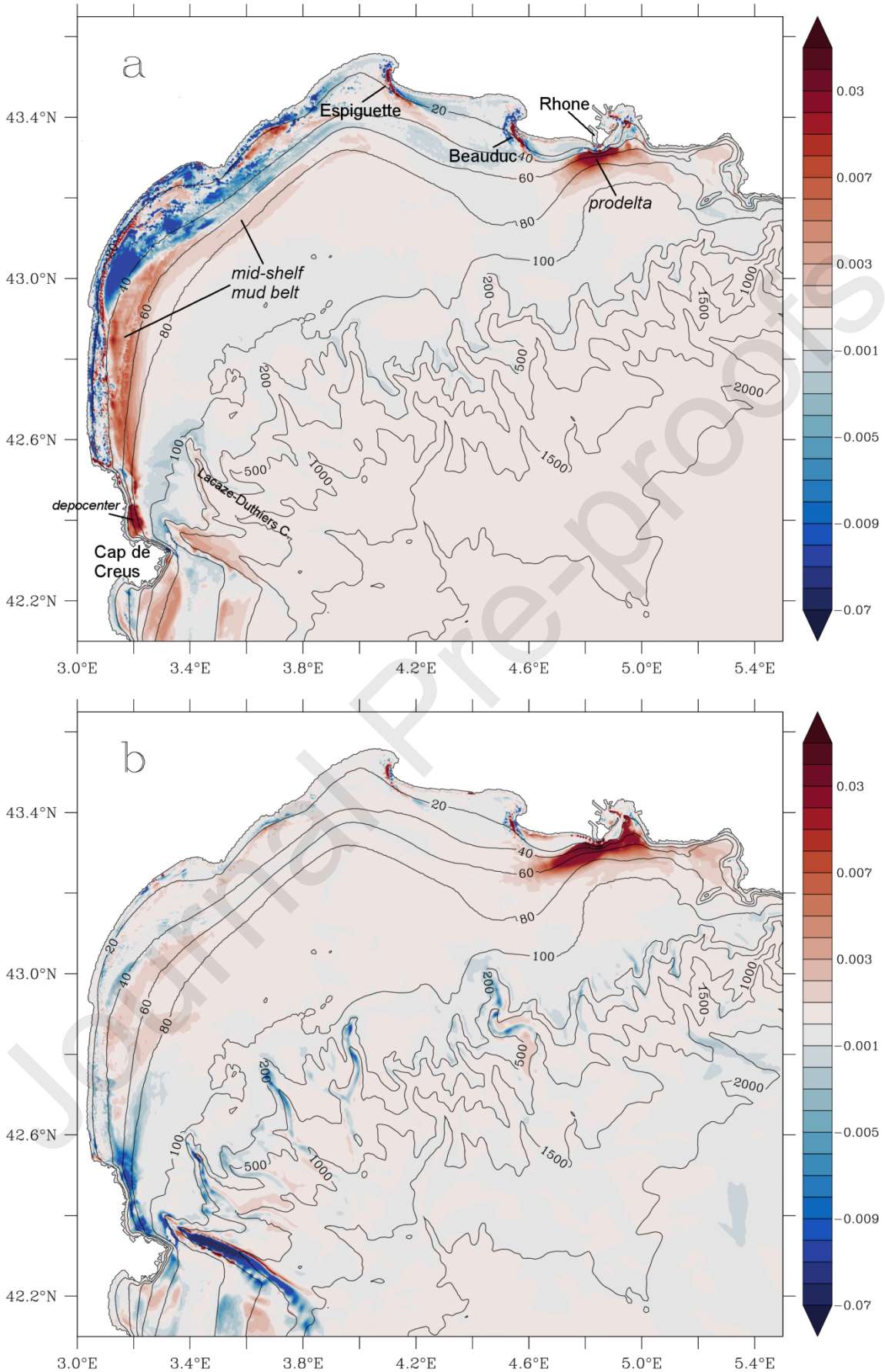

Figure 10. Thickness of deposition (positive) and erosion (negative) in meters between 15 September and 15 April in (a): 2010-2011 and (b): 2011-2012. Note the change in color spacing: 1 mm between -1 cm and +1 cm and 2 cm below -1 cm and above +1 cm.

The chronology of the inputs by all the rivers of the Gulf of Lion, and of the deposition on the shelf beyond the Rhone extended prodelta (mapped in Fig. 8) presented in Figure 11, highlights the major role of storms and floods on shelf sediment. Different bathymetric slices have been chosen: the entire shelf delimited here by the 100 m isobath, the inner shelf between 0 and 40 m and the mid-shelf mud belt between 40 and 80 m of water depth.

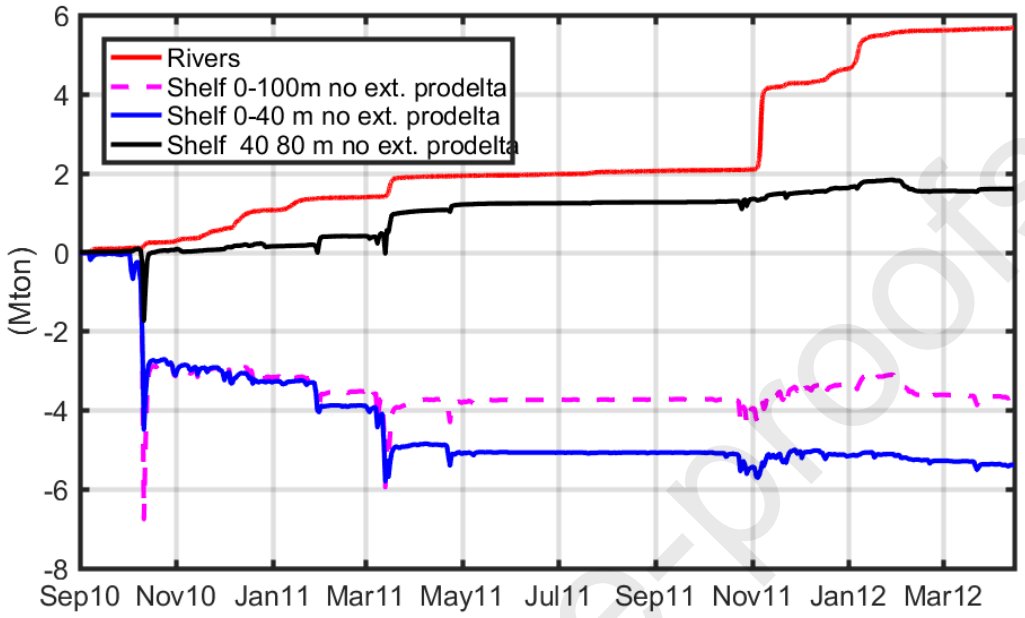

Figure 11. Deposition integrated over the continental shelf (bathymetry<100 m and latitude>42.6 °N and outside the extended Rhône prodelta) and by bathymetric slices. Values are counted since the start of the simulation (31 August 2010).Rivers discharge are accumulated since the start of the simulation.

The entire shelf outside the extended Rhone prodelta (magenta dotted line in Fig. 11) lost 3.7 Mt during the whole period. Its chronology, which is close to that of the inner shelf (here 0-40 m, blue line in Fig. 11), is marked by the two storms of October 2010 and March 2011. In October 2010, 6 Mt of sediment were resuspended in 2 days and only 3.7 Mt were deposited again in the following 3 days, the deficit reflecting a massive southwestward export (not shown). On the contrary, during the March 2011 storm, the 2.3 Mt resuspended were almost totally redeposited on the shelf.

The mid-shelf mud belt between 40 and 80 m depth (black line in Fig. 11) gained 1.6 Mt during the whole period. This gain was focused between November and March periods. The mid-shelf belt dynamics is governed by two types of situations: feeding by riverine inputs, and feeding by resuspension over the inner shelf during some storms, as in winter 2011 (i.e. end of January and March). Certain storms such as in October 2010, and even more weakly the event preceding the flood of November 2011, have a weak net impact with resuspension and deposition following each other a few days apart. The area between 80 and 100 m accumulates a low amount of sediment (0.12 Mtons), thus the evolution of deposition in this area is not shown.

Concerning the specific role of the Rhone River, its impact on the accretion of the 40-80 m mid-shelf mud belt (black line) appears certain. However, this impact does not seem to quickly reflect the rapid timing of the major floods of November 2011 and January 2012, as does the extended prodelta evolution (Fig. 9). Fig. 11 shows a slow response of the sediment of the mud belt attributed to the slow sedimentation of the finest particles.

5.3 Spatial and temporal variability of sediment dynamics on the slope

The sediment erosion and accumulation on the slope are also much contrasted between the two years. The major impacts are in the canyons and are dominant in the second year (Fig. 10b). The

western flanks of the canyons that incise the shelf to 120 m deep (i.e., Lacaze-Duthiers, Bourcart/Aude, Hérault, Petit Rhône canyons), underwent significant erosion beyond the 500 m isobath (Fig. 10b). Figure 12 is a refinement of Figure 10 that focuses on the exit of the Gulf of Lion to the southwest, with an extension further south to the North Catalan shelf also incised by a canyon, the Palamos Canyon whose sedimentary functioning has been the subject of various observations (Palanques et al., 2005; Ribó et al., 2011). The bottom current averaged over the 7 months of each period has been superimposed on the sediment height variation in this figure. A highlight of the first year is the deposition of a few millimeters of sediment in the Cap de Creus and the Palamos Canyons between 400 and 700 m depth (Fig. 12a). The upper reaches of these two canyons are therefore prime outlets for storm-eroded sediment. In the second year, the Cap de Creus Canyon experienced a very strong erosion induced by the cascading currents (Fig. 12b). Erosion extended along the canyon axis (slightly offset on the southern flank) and down to 1500 m deep. The amounts of eroded sediment were larger than those deposited in the first year. It should be noted however that the amounts of sediment eroded along the dense water vein inside the Cap de Creus Canyon are uncertain as they should depend on the initialization of sediment properties that do not reproduce the actual complex structure of consolidated sediments, rocky outcrops and temporary deposits (Canals et al., 2006; Lastras et al., 2007; DeGeest et al., 2008). Canals et al. (2006) and Puig et al. (2008) already highlighted the impact of cascading in this canyon during the winter of 2005, which triggered erosion of unconsolidated sediment, the development of erosional landforms on consolidated mud such as 100 m wavelength furrows, likely by sand blasting, and finally the transport of heavy loads of sediment downcanyon. As the dense water cascading event simulated here for winter 2012 is of comparable magnitude to the one of 2005 (Durrieu de Madron et al., 2013), such impacts likely occurred as well. Our results are in line with these impacts with respect to: (i) erosion of deposits accumulated during the previous winter's storms in the southwestern part of the Gulf of Lion shelf and in the upper part of the Cap de Creus Canyon; and (ii) erosion along the canyon. The eroded area in the canyon is bordered on either side by a narrow band of strong deposition discussed in section 5.4. The similarity of the behavior of the Cap de Creus and Palamos canyons during the storm-dominated period is no longer true for cascading. Erosion in the Palamos Canyon was restricted to a narrow band around 500 m depth. This erosion probably fed the deposit deeper in the canyon (down to 1500 m) than during the first year. The recurrent presence of cascading in the Palamos Canyon is attested by Ribó et al. (2011) who noted that the amount of sediment transported during the moderate cascading events of 2007 and 2008 was one order of magnitude lower than in the Cap de Creus Canyon. This is consistent with the difference between the erosion patterns simulated here in the two canyons.

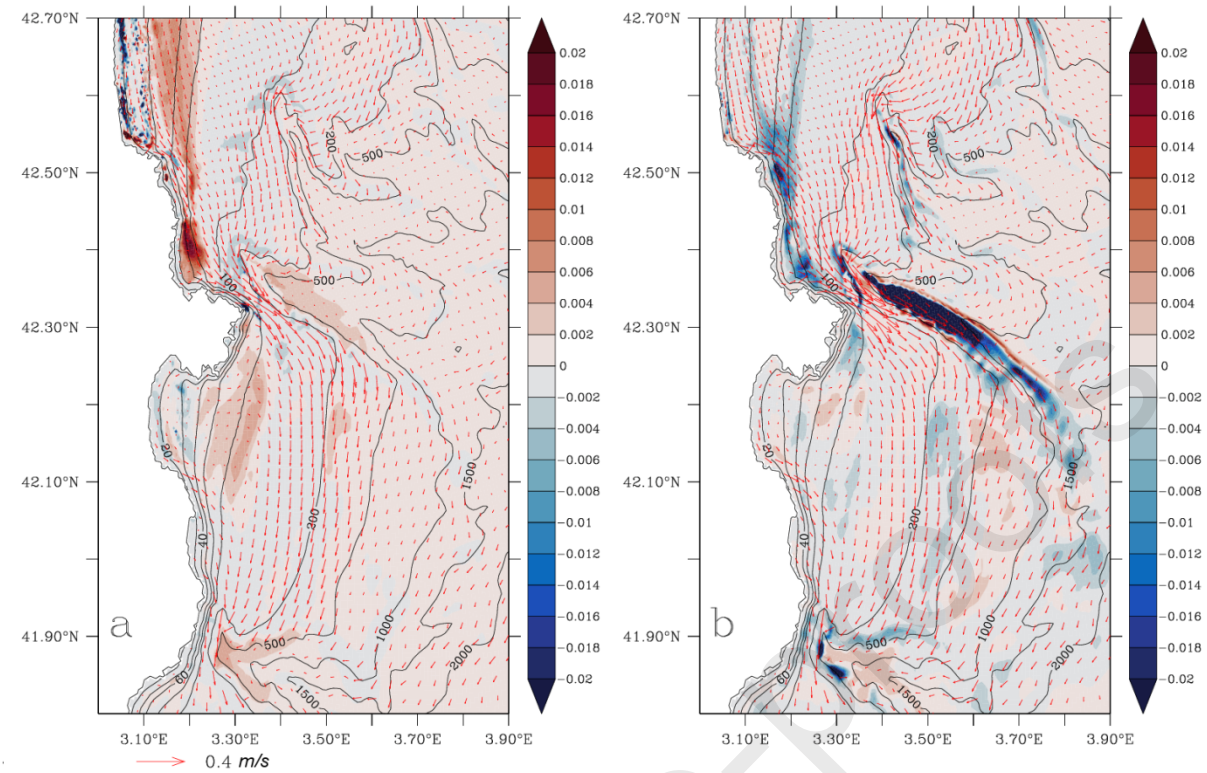

Figure 12. Thickness of sediment deposition (positive) and erosion (negative) in meters between 15 September and 15 April in the southwestern Gulf of Lion and on the Catalan margin in (a): 2010-2011, and (b): 2011-2012. The bottom current averaged over the same periods have been superimposed.

On the open slope between the two canyons, successive along-isobath deposition and erosion zones appeared during the second period (Fig. 12b). This is coherent with the observation during the 2006 cascading of turbid dense shelf water which had overflowed the Cap de Creus Canyon walls beyond 1000 m depth and had a dominant along-slope southwards component to the Palamos Canyon (Palanques et al., 2012). Such an overflow is evidenced in Fig. 12b by an erosional band that detaches from the main band inside the canyon, and exits along the 500 m isobath on its southern flank. Once outside the canyon, the dense water vein tends to slow down because the bathymetric slope is weaker than inside the canyon. Depending on the current speed at the exit of the canyon, erosion can continue for a few kilometers or, on the contrary, rapid deposition can occur if the dense water vein is loaded with coarse sediments that the flow can no longer maintain in suspension.

5.4 Dynamics of sand and mud

The migration of sand and mud from the beginning to the end of the simulated period is displayed in Figure 13 a,b respectively. The accretion zones visible around the Beauduc and Espiguette spits (Fig. 10) are fed mainly by sand (Fig. 13a). The thin band of sand accumulation against the coast between Beauduc and the Rhone mouth corresponds to the deposition of the “less stormy” second year (Fig. 10b) and is therefore probably temporary. More generally, most areas between 0 and 20 m depth were eroding in sand (Fig. 13a). In detail (not shown), the sorting of the two sand classes is obvious with medium sands along the coastline and fine sands beyond the 20 m isobath. To the north, between Beauduc and Espiguette spits, the sand erosion zone reaches 30-40 m in depth reflecting the strong bottom stresses characterizing this region, and which also inhibit fine sediment deposition. The result is the discontinuity in the deposits shown in Fig. 10a between the extended Rhone prodelta and the mid-shelf mud belt west of 4°E. To the west, the erosion of nearshore sands feeds the 20-40 m band (Fig. 13a). This is consistent with Brunel et al. (2014) who noted a negative sediment budget of the shoreface in the last decades, six times stronger than during the previous century, suggesting that these losses feed the greater depths. As suggested in Figure 10, these sand displacements occur during the first period and are therefore storm-induced.

Undoubtedly, it is the second period cascading that produces displacements of relict sands (much weaker than the displacements of inner-shelf sands), from the shelf edge, upper slope and canyon heads to deeper places in the canyons. They appear generally as two elongated depositional features (Fig. 13a) probably marking the dense water vein edges where deposition is enabled by weaker currents. This sand deposition is 2 cm thick in the Cap de Creus Canyon, where the dynamics related to cascading is much stronger than in the other canyons. Furthermore, we note that in the Cap de Creus Canyon head (between the 200 and 500 m isobaths), cascading produces a sand deposit which is consistent with the high sand content (61%) found during this event in the sediment trap located 25 m above the bottom at 300 m depth (Sanchez-Vidal et al., 2015). The band of sand, parallel to the Cap de Creus Canyon downstream from the canyon to the south, indicates as suggested above, deposition of the sand eroded inside the canyon once the dense water vein overflows the canyon and slows down. This overflow can occur at different depths during the cascading period depending on the variable water mass density as suggested by the spread of this deposit.

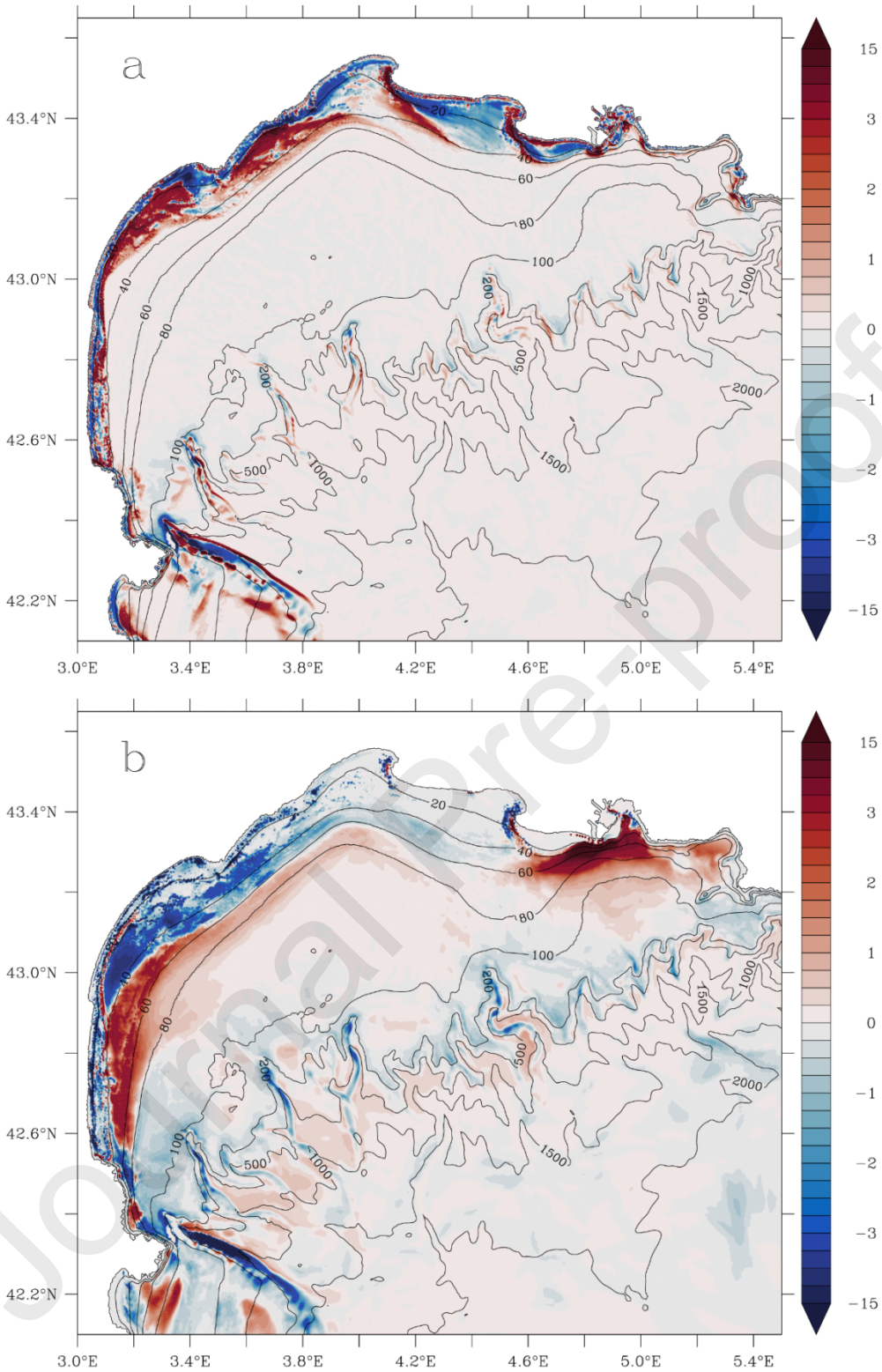

Figure 13. Mass balance in kg m^{-2} of (a): sand and (b): mud in the Gulf of Lion over the whole simulation period. Note the shift in scales below -3 and above +3 kg m^{-2}

Concerning mud deposition, the extended Rhone prodelta and the mid-shelf mud belt, previously discussed, are the major features on the shelf (Fig. 13b). The small accumulation zone close to the coast at 42.4°N already noted is composed of mud and is separated from the mid-shelf mud belt by a no-deposit zone between 42.45 and 42.55°N. This depositional geometry is strictly consistent with the observations of DeGeest et al. (2008) who referred to the no-deposit zone as the "Middle shelf zone of Bypassing" and attributed it to the acceleration of the flow due to the presence of Cap Bear. A kind of mid-shelf mud belt south of the Cap de Creus promontory in front of Rosas Bay is also simulated.

On the continental slope, we note a cascading-induced erosion of the mud accumulated rather on the western flanks of the canyons with, as for sands, a much greater extent in the Cap de Creus Canyon. On the other hand, mud deposits following erosion within the Cap de Creus Canyon are less marked than those of the sand but equally localized on both sides of the main erosion channel. The relative weakness of mud deposit likely reflects dispersion at larger distances as related to lower sedimentation rates (Puig et al., 2013).

5.5 Sediment budget of the Gulf of Lion continental shelf

The sediment budget of the Gulf of Lion continental shelf (bathymetry < 100m) over the simulation period is presented in Figure 14. River inputs account for nearly 6 Mt (4.3 Mt for the Rhone River alone), and sediment loses 1.3 Mt. This involves an export to the slope (bathymetry > 100 m) and southwards to the North Catalan margin of 7 Mt. We have seen that the extended Rhone prodelta on the other hand has accreted 2.4 Mt (56% of the Rhone input). The deficit of the shelf concentrates therefore outside this region and more precisely on the 0-40 m depth band (Fig. 11). We also considered the sand exported from the shelf to the slope (not shown): if we place the shelf/slope boundary at 100 m depth, the sand export is 0.12 Mt while if the boundary is positioned at 200 m, the export increases to 0.41 Mt of which 70% took place during the cascading event of the second year. This confirms that the exported sands are relict sands from the outer shelf which are mostly transferred by cascading as inferred by Gaudin et al. (2006) from analyses of interface cores in the Bourcart Canyon.

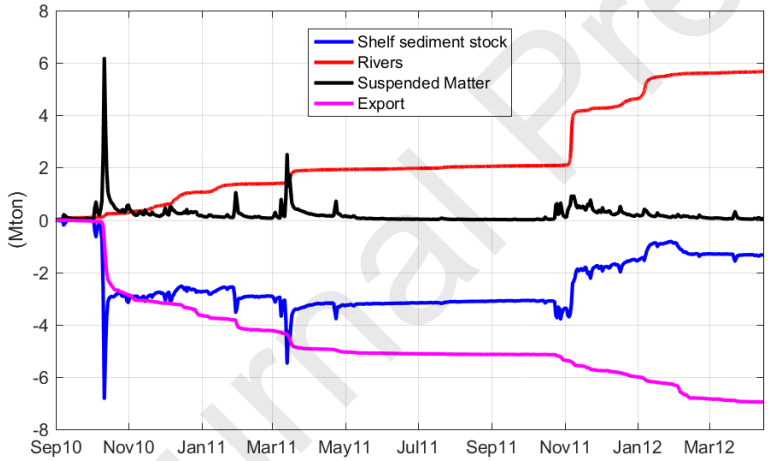

Figure 14. Particulate matter budget (Mt) of the Gulf of Lion shelf (h<100 m). River input and suspended matter are counted as positive. River input and export are accumulated since the beginning of the simulation (31 August 2010).

Table 3 lists the most significant storms and their impact on sediment dynamics. The selection criterion is the significant wave height simulated to the west (POEM buoy) and to the north (off the Rhone River mouth) of the Gulf of Lion. An analysis of the different storms encountered over the two years allowed us to estimate a threshold of 2.8 m of significant wave height at 20 – 30 m depth leading to significantly displacement of the sediment. The events in Table 3 are those for which the wave height (sampled at 30 minutes interval) exceeds 2.8 m at least once at either site. The periods when shelf sediment are the most detrimentally impacted coincide with significant storm periods, in particular with the October 2010 and then March 2011 storms when a loss of 2.8 and 0.5 Mt (88% and 16% of the net deficit of year 1) is found. However It should be noted that during the two storms associated with concomitant flood of the Rhone, occurring in Nov - Dec 2010 and Oct - Nov 2011 riverine inputs compensate or even exceed sediment exports (net gain of 1.2 Mt during the Oct. Nov 2011 storm). During these two episodes, the waves in the southwestern Gulf of Lion (POEM buoy) were significantly lower than in the north. Since the resuspension areas are far from the shelf outlet, this type of situation could be less favorable for export than the reverse conditions or when the waves

are high over the whole Gulf. This effect should be verified through a longer simulation period including more events.

Storm period	Presence of flood	H_s (m) (POEM-Rhone)	Shelf budget (Mt)	Prodelta budget (Mt)
Oct 10-11 2010	Yes (Small Riv.)	4. – 2.8	-2.8	+0.14
Nov 30-Dec 1 2010	Yes	1.8 – 3.4	~0	+0.24
Jan 29 2011	No	2.8 – 2.6	-0.3	~0
Mar 12-15 2011	Yes (Small Riv.)	3.5 – 3.6	-0.5	-0.1
Oct 24-Nov 5 2011	Yes	2.1 – 3.4	+1.2	+1.1
Year 1	/	/	**-3.2**	**+0.6**
Year 2	/	/	**+1.9**	**+1.7**

Table 3. Characteristics of the strongest storms (see text for criterion) and impact on the sediment of the shelf and prodelta. The sediment budget for the two annual periods is also recalled.

6. Conclusions

We present for the first time a modeling of sediment transport on the Gulf Lion shelf and slope over a period including two succeeding autumn/winter seasons. The results of the numerical simulation presented here are consistent with current knowledge of the long-term (typically centennial) characteristics of the shelf sediment dynamics which are: (1) the massive storage of sediment off the Rhone mouth; (2) the accretion of the mid-shelf mud belt; (3) the orders of magnitude of accumulation rates off the Rhone mouth and on the whole shelf.

This study provides new insight on the sediment dynamics in the Gulf of Lion considering from river's discharge to shelf/slope export, subsequently illustrating both the spatial and temporal variability of deposition and erosion, and distinguishing the major morphosedimentary zones. The marked differences between two autumn-winter periods make it possible to apprehend the variability of sediment dynamics over the Gulf of Lion shelf and the meteo-oceanic drivers behind.

The first period is marked by numerous marine storm and swell events and weak dense water formation and cascading whereas the second one encompasses few marine storms, a major flood of the Rhone River and intense formation and cascading of dense shelf water. The two active periods (October to March) from the sediment dynamics viewpoint show radically different behaviors, which relate to the recurrence and response of the system to storms and cascading. During the first period (2010-2011), shelf sediment changes were shaped by storms with: (1) major deposits from the Rhone River sediment accumulating in a relatively small area; (2) the inner shelf mud loss feeding the mid-shelf mud belt; (3) the feeding of the uppermost reach of the Cap de Creus Canyon by the storm-triggered downwelling events; and (4) the southward export of the sediment to the North Catalan shelf south of the Gulf of Lion. The analysis of the different storms encountered allowed estimating a threshold of 2.8 m of significant wave height at 20 - 30 m depth leading to significantly sediment remobilisation. During the less stormy and colder period (2011-2012), the sediment cover on the shelf underwent very few changes except for: (1) the extended Rhone prodelta whose area increased due to two major floods and the scarcity of swell events which helped preserving the deposits; (2) the erosion at the southwestern end of the Gulf of Lion, where gravity currents related to the cascading of dense shelf water were particularly strong and led to seabed erosion. These gravity currents also impacted the sediment in the canyons incising the Gulf's continental shelf.

The simulated 2010-2012 period therefore illustrates a high interannual variability of the sediment

dynamics in the Gulf of Lion, as well as a form of "complementarity" between the two simulated years to promote the export of particulate matter from the shelf to greater depths: repeated storms causing thick deposits in the southwestern shelf and in the upper part of the Cap de Creus Canyon; deep cascading occurring more rarely but driving these deposits towards the deepest canyon reaches and likely beyond.

With, on the one hand, an amount of matter exported from the shelf close to the rivers supplies and, on the other hand, storage of about half of the supplies of the Rhone near its mouth, it is clear that the rest of the shelf is sediment-starved under current conditions, especially the inner shelf —despite the thick littoral prism that formed in the longer term (Berné et al., 2004; Labaune et al., 2005)— as the mid-shelf mud belt is itself in accretion. We consider this point as a major outcome that arises from our results. It should be noted that glider and satellite observations confirm the very strong sediment dynamics of the inner shelf during storms with (1) high SPM concentrations and intense vertical mixing that extends up to the sea surface thus delaying deposition, and (2) strong currents typical of storm periods pointing, in accordance with the simulations, to an efficient transfer of fine resuspended particulate matter towards the southwestern end of the Gulf of Lion, thus supplying most of the export of shelf sediment. An emerging issue here is the long-term persistence of this mechanism that tends to deplete the inner shelf of the fine fractions. A longer simulation period would allow understanding whether this is a real trend or a particularity of the simulated period, and whether other processes can make it possible to recharge the internal shelf with fine sediments. It would be interesting, for example, to consider the impact of another year of strong storms on the Rhone deposits of the second period studied here, including the depositional patches located at 10 - 20 m depth. It is likely that parts of these deposits would be resuspended and transferred westward. This mechanism could at least partially replenish the stock of fine sediments on the inner shelf.

The modeling here applied, involves several uncertainties. The sedimentary module in particular is based on numerous parameterizations and simplifications. For this reason, some processes are not explicitly represented, such as flocculation, consolidation, bioturbation or bed load transport, which could be significant in canyons. The consideration of these processes or sophistication of their formulations could be added to the model. For example, sand transport is a weak part of the model that will require more attention in the future. The settling velocities of the fine sediments have a considerable importance on the results of the model. A choice has been made here by stating an univocal distribution of suspended matter between primary particles and flocs regardless of the concentrations of suspended matter, the physical, chemical or biological conditions. Another strategy could be using flocculation models dedicated to some of these processes. However, the likely complexity of this process in the presence of multiple drivers led us to prefer more simplistic empirical relationships that were adjusted during the calibration phase to best represent the time series of observed suspended matter. By keeping this empiricism (which also allows reducing the computation time), a reduction of the uncertainties would require constraining by more observations. Observing suspended matter at the shelf spatial scale and on seasonal time scales remains a complex challenge that only satellites and autonomous platforms such as gliders can currently meet, each of them with their own limits and uncertainties. Further exploiting the satellite observations already available and intensifying glider deployments is probably the main avenue for improving our simulations.

Our work supports the notion of an unbalanced sedimentary system with a major driver being the reduction of the particulate matter supplies from the Rhone by a factor of 4 in less than a century. The regime and discharge of the smaller rivers of the west coast have also been modified by human intervention. The acceleration of shoreline erosion in the Rhone delta and more generally along the entire coast of the Gulf of Lion is an indication of the cross-shore displacement of littoral sands. In a complementary way, our results indicate a transfer of fine sediments from the inner shelf to the mid-shelf and ultimately to the deep margin and basin.

In order to verify our results and project them into the future, longer simulations (at least at decadal scale) should be carried out to increase the diversity of events into consideration, and to obtain a refined sediment budget that is representative of current conditions. Secondly, there should be a

focus on sediment dynamics change in the Gulf of Lion along the 21st century, taking into account alterations in climatic and anthropogenic driving factors such as: increase of extreme precipitation events and therefore, of the frequency of floods (Tramblay and Somot, 2018); milder marine storms and lowered wave height (Lionello et al., 2008; Kapelonis et al., 2015); strong reduction of dense water volumes formed on the shelf and lessening of cascading frequency and intensity (Herrmann et al., 2008). A decrease in storm intensity would tend to favor sediment storage in the Rhone prodelta while cascading collapse would enhance sediment transport towards the North Catalan shelf, instead of the slope or deep basin, or even burial over the long term in the upper part of the Cap de Creus Canyon. A dedicated study based on a carefully calibrated model will therefore be very welcome to assess all the consequences of the modification of the different drivers of sediment dynamics over the Gulf of Lion continental shelf, and of other shelves all over the world.

Acknowledgments

Authors would like to thank André Monaco for sharing, many years ago, his knowledge and enthusiasm for the subject of this article. CE also thanks Pierre Le Hir and Bénédicte Thouvenin for their help and advice on using the Mustang model. This study (including the PhD and Postdoc of G. Mikolajczak) was mainly funded by the AMORAD-project (grant ANR-11-RSNR-0002 of the French program Investissement d'Avenir run by the Agence Nationale de la Recherche). We also benefited from the support of the CHIFRE and DeltaRhone projects of the national EC2CO program. The simulations were performed using HPC resources from CALMIP (Grant P09115) and CINES OCCIGEN (Grant A0040110088). This research was also supported by grant PID2020-114322RB-I00 (FAR-DWO) funded by MCIN/AEI/ 10.13039/501100011033.

REFERENCES

Aloisi, J.C., Got, H., Monaco, A., 1973. Carte géologique du précontinent languedocien au 1/250000ième. International Institute for Aerial Survey and Earth Sciences (I.T.C.) (Eds.), Netherlands.

Aloisi, J.C., Millot, C., Monaco, A., Pauc, H., 1979. Dynamique des suspensions et mécanismes sédimentologiques sur le plateau continental du Golfe du Lion. C. R. Acad. Sci., Paris 289, 879 – 882.

Antonelli, C., Eyrolle, F., Rolland, B., Provansal, M., Sabatier, F., 2008. Suspended sediment and ^{137}Cs fluxes during the exceptional December 2003 flood in the Rhone River, southeast France, Geomorphology, 95, 3–4, 350-360, https://doi.org/10.1016/j.geomorph.2007.06.007

Appleby, P.G., Oldfield, F., 1983. The assessment of ^{210}Pb data from sites with varying sediment accumulation rates. Hydrobiologia 103, 29–35. https://doi.org/10.1007/BF00028424

Appleby, P. G., 1998. Dating recent sediments by ^{210}Pb: Problems and solutions. STUK-A--145. https://www.osti.gov/etdeweb/servlets/purl/660408

Bassetti, M.-A., Jouet, G., Dufois, F., Berné, S., Rabineau, M., Taviani, M., 2006. Sand bodies at the shelf edge in the Gulf of Lions (Western Mediterranean): Deglacial history and modern processes. Marine Geology 234, 93–109.

Berné, S., Carré, B., Loubrieu, B., Mazé, J.P., Morvan, L., Normand, A.,2004. Le Golfe du Lion, Carte morpho-bathymétrique, Ifremer, Brest, France.Boudet, L., Sabatier, F., Radakovitch O., 2017. Modelling of sediment transport pattern in the mouth of the Rhone delta: Role of storm and flood events. Estuarine, Coastal and Shelf Science 198 (2017) 568-582.

Bourrin, F., Durrieu de Madron, X., Heussner, S., Estournel, C., 2008. Impact of winter dense water formation on shelf sediment erosion (evidence from the Gulf of Lions, NW Mediterranean). Continental Shelf Research, 28, 1984– 1999. doi:10.1016/j.csr.2008.06.006

Bourrin, F., Many, G., Durrieu de Madron, X., Martín, J., Puig, P., Houpert, L., Testor, P., Kunesch, S., Mahiouz, K., Béguery, L., 2015. Glider monitoring of shelf suspended particle dynamics and transport during storm and flooding conditions. Continent. Shelf Res. 109, 135–149. https://doi.org/10.1016/j.csr.2015.08.031

Brunel, C., Certain, R., Sabatier, F., Robin, N., Barusseau, J.P., Aleman, N., Raynal, O., 2014. 20th century sediment budget trends on the Western Gulf of Lions shoreface (France): An

application of an integrated method for the study of sediment coastal reservoirs, Geomorphology 204, 625-637, https://doi.org/10.1016/j.geomorph.2013.09.009

Calmet, D., Fernandez, J.M., 1990. Caesium distribution in northwest Mediterranean seawater, suspended particles and sediments. Continental Shelf Research 10 (9–11), 895-913, https://doi.org/10.1016/0278-4343(90)90066-U

Canals, M., Puig, P., Durrieu de Madron, X., Heussner, S., Palanques, A., Fabres, J., 2006. Flushing submarine canyons. Nature 444, 354–357.

Charmasson, S., Radakovitch, O., Arnaud, M., Bouisset, P., Pruchon, A.-S., 1998. Long-core profiles of ^{137}Cs, ^{134}Cs, ^{60}Co and ^{210}Pb in sediment near the Rhône river (northwestern Mediterranean Sea). Estuaries, 21 (3), 367-378.

Charmasson, S., 2003. ^{137}Cs inventory in sediment near the Rhone mouth: role played by different sources, Oceanologica Acta, 26, 435-441, https://doi.org/10.1016/S0399-1784(03)00036-7

Chassefiere, B. 1990. Mass-physical properties of surficial sediments on the Rhone continental margin: Implications for the nepheloid benthic layer. Continental Shelf Research 10:857-868.

Curran, K., Hill, P., Milligan, T., Mikkelsen, O., Law, B., Durrieu de Madron, X., Bourrin, F., 2007. Settling velocity, effective density, and mass composition of suspended sediment in a coastal bottom boundary layer, Gulf of Lions, France. Cont. Shelf Res. 27, 1408–1421.

DeGeest, A.L., Mullenbach, B.L., Puig, P., Nittrouer, C.A., Drexler, T.M., Durrieu de Madron, X., Orange, D.L., 2008. Sediment accumulation in the western Gulf of Lions, France: The role of Cap de Creus Canyon in linking shelf and slope sediment dispersal systems. Cont. Shelf Res. 28: 2031-2047. https://doi.org/10.1016/j.csr.2008.02.008

Dufois, F., Garreau, P., Le Hir, P., Forget, P., 2008. Wave- and current-induced bottom shear stress distribution in the Gulf of Lions. Cont. Shelf Res. 28, 1920–1934. http://dx.doi.org/10.1016/j.csr.2008.03.028

Dufois, F., Verney, R., Le Hir, P., Dumas, F., Charmasson, S., 2014. Impact of winter storms on sediment erosion in the Rhone River prodelta and fate of sediment in the Gulf of Lions (North Western Mediterranean Sea). Continental Shelf Research 72, 57–72. http://dx.doi.org/10.1016/j.csr.2013.11.004

Durrieu de Madron, X., Abassi, A., Heussner, S., Monaco, A., Aloisi, J.C., Radakovitch, O., Giresse, P., Buscail, R.,Kerherve, P., 2000. Particulate matter and organic carbon budgets for the Gulf of Lions (NW Mediterranean). Oceanologica Acta 23, 6, 717-730.

Durrieu de Madron, X., Ferré, B., Le Corre, G., Grenz, C., Conan, P., Pujo-Pay, M., Buscail, R., Bodiot, O., 2005. Trawling-induced resuspension and dispersal of muddy sediments and dissolved elements in the Gulf of Lions (NW Mediterranean). Continental Shelf Research, 25, 2387–2409.

Durrieu de Madron, X., Wiberg, P.L., Puig, P., 2008. Sediment dynamics in the Gulf of Lions: The impact of extreme events. Continental Shelf Research, 28: 1867-1876

Durrieu de Madron, X., et al., 2013. Interaction of dense shelf water cascading and open-sea convection in the northwestern Mediterranean during winter 2012, *Geophys. Res. Lett.* 40, 1379– 1385, doi:10.1002/grl.50331

Dyer, K.R., 1986. Coastal and Estuarine Sediment Dynamics. Wiley,Chicherster.

Estournel, C., Kondrachoff, V., Marsaleix, P., Vehil, R., 1997. The plume of the Rhone: numerical simulation and remote sensing. Continent. Shelf Res. 17, 899–924. https://doi.org/10.1016/S0278-4343(96)00064-7

Estournel, C., Durrieu de Madron, X., Marsaleix, P., Auclair, F., Julliand, C., Vehil, R., 2003. Observation and modeling of the winter coastal oceanic circulation in the Gulf of Lion under wind conditions influenced by the continental orography (FETCH experiment). Journal of Geophysical Research: Oceans 108 (C3), 8059. https://doi.org/10.1029/2001JC000825

Fanget, A.S., Bassetti, M.A., Arnaud, M., Chiffoleau, J.F., Cossa, D., Goineau, A., Fontanier, C., Buscail, R., Jouet, G., Maillet, G.M., Negri, A., Dennielou, B., Berné, S., 2013. Historical evolution and extreme climate events during the last 400 years on the Rhone prodelta (NW Mediterranean). Marine Geology 346, 375–391. doi:10.1016/j.margeo.2012.02.007

Fernandez, J. M., Badie, C., Zhen, Z. & Arnal, I., 1991. Le ^{137}Cs: traceur de la dynamique sédimentaire sur le prodelta du Rhône Méditerranée Nord Occidentale. In Radionuclides in the Study of Marine Processes (Kershaw, P. J. & Woodhead, D. S., eds). Elsevier, London & New

York, pp. 197–208.

Ferré, B., Durrieu de Madron, X., Estournel, C., Ulses, C., Le Corre, G., 2008. Impact of natural (waves and currents) and anthropogenic (trawl) resuspension on the export of particulate matter to the open ocean: application to the Gulf of Lion (NW Mediterranean). Cont. Shelf Res. 28, 2071–2091. http://dx.doi.org/10.1016/j.csr.2008.02.002

Gangloff, A., 2017. Devenir des apports solides du Rhône dans le Golfe du Lion : étude de la dynamique du panache turbide du Rhône en réponse aux forçages hydrométéorologiques. Thèse Université de Brest. https://tel.archives-ouvertes.fr/tel-01797368/document

Gangloff, A., Verney, R., Doxaran, D., Ody, A., Estournel, C., 2017. Investigating Rhône river plume (Gulf of Lions, France) dynamics using metrics from the MERIS 300m Ocean Color archive (2002-2012), Continental Shelf Research, 144, 98-111, https://doi.org/10.1016/j.csr.2017.06.024

Gaudin, M., Berné, S., Jouanneau, J.-M., Palanques, A., Puig, P., Mulder, T., Cirac, P., Rabineau, M., Imbert, P., 2006. Massive sand beds attributed to deposition by dense water cascades in the Bourcart canyon head, Gulf of Lions (northwestern Mediterranean Sea), Marine Geology, 234, 1–4,111-128, https://doi.org/10.1016/j.margeo.2006.09.020

Gentil, M ., C. Estournel, X. Durrieu de Madron, G. Many, T. Miles, P. Marsaleix, S. Berné, F. Bourrin, 2022. Sediment dynamics on the outer-shelf of the Gulf of Lions during an onshore storm: an approach based on acoustic glider and numerical modelling. Continental Shelf Research, 240, 104721,https://doi.org/10.1016/j.csr.2022.104721.

Got, H., Aloisi, J., 1990. The Holocene sedimentation on the Gulf of Lions margin: a quantitative approach. Continental Shelf Research 10, 841–855.

Guillén, J., Bourrin, F., Palanques, A., Durrieu de Madron, X., Puig, P., Buscail, R., 2006. Sediment dynamics during wet and dry storm events on the Têt inner shelf (SW Gulf of Lions). Mar. Geol. 234, 129–142. http://dx.doi.org/10.1016/j.margeo.2006.09.018

Herrmann M., Estournel C., Déqué M. , Marsaleix P., Sevault F., Somot S., 2008, Dense water formation in the Gulf of Lions shelf: Impact of atmospheric interannual variability and climate change, Continental Shelf Research, 28, 2092-2112.

Kapelonis, Z.G., Gavriliadis, P.N., Athanassoulis, G.A., 2015. Extreme Value Analysis of Dynamical Wave Climate Projections in the Mediterranean Sea, Procedia Computer Science, 66, 210-219, https://doi.org/10.1016/j.procs.2015.11.025.

Labaune, C., Tesson, M., Gensous, B., 2005. Integration of High and Very High-resolution Seismic Reflection Profiles to Study Upper Quaternary Deposits of a Coastal Area in the Western Gulf of Lions, SW France. Marine Geophysical Researches 26, 109-122. https://doi.org/10.1007/s11001-005-3711-z.

Lansard, B, Charmasson, S., Gascó, C..Antón, M.P., Grenz, C., Arnaud, M., 2007. Spatial and temporal variations of plutonium isotopes (^{238}Pu and ^{239,240}Pu) in sediments off the Rhone River mouth (NW Mediterranean). Science of The Total Environment 376, 1–3, 215-227. https://doi.org/10.1016/j.scitotenv.2007.01.069

Lastras, G., Canals, M., Urgeles, R., Amblas, D., Ivanov, M., Droz, L., Dennielou, B., Fabrés, J., Schoolmeester, T., Akhmetzhanov, A., Orange, D., García-García, A., 2007. A walk down the Cap de Creus canyon, northwestern Mediterranean Sea: Recent processes inferred from morphology and sediment bedforms. Marine Geology, 246 **(**2-4), 176-192. Doi: 10.1016/j.margeo.2007.09.002.

Le Hir, P., Cayocca, F., Waeles, B. Dynamics of sand and mud mixtures: A multiprocess-based modelling strategy. Cont. Shelf Res. 2011, 31, S135–S149.

Lionello, P., Cogo, S., Galati, M.B., Sanna, A., 2008. The Mediterranean surface wave climate inferred from future scenario simulations, Global and Planetary Change, 63, 2–3, 152-162, https://doi.org/10.1016/j.gloplacha.2008.03.004.Maillet, G., Vella, C., Berné, S., Friend, P.L., Amos, C.L., Fleury, T.J., Normand, A., 2006. Morphological changes and sedimentary processes induced by the December 2003 flood event at the present mouth of the Grand Rhône River (southern France). Mar. Geol. 234 (1–4), 159–177.

Many, G., Bourrin, F., Durrieu de Madron, X., Pairaud, I., Gangloff, A., Doxaran, D., Ody, A., Verney, R., Menniti, C., Le Berre, D., Jacquet, M., 2016. Particle assemblage characterization in the Rhone River ROFI. J. Mar. Syst., 157, 39-51, 10.1016/j.jmarsys.2015.12.010

Many, G., Bourrin, F., de Madron, X.D., Ody, A., Doxaran, D., Cauchy, P., 2018. Glider and satellite monitoring of the variability of the suspended particle distribution and size in the Rhône ROFI. Progress in oceanography 163, 123–135.

Many, G., Durrieu de Madron, X., Verney, R., Bourrin, F., Renosh, P.R., Jourdin, F., Gangloff, A., 2019. Geometry, fractal dimension and settling velocity of flocs during flooding conditions in the Rhône ROFI. Estuarine, Coastal and Shelf Science 219, 5, 1-13.

Many, G., Ulses, C., Estournel, C., Marsaleix, P., 2021. Particulate organic carbon dynamics in the Gulf of Lion shelf (NW Mediterranean) using a coupled hydrodynamic–biogeochemical model, Biogeosciences, 18, 5513–5538, https://doi.org/10.5194/bg-18-5513-2021

Marion, C., Dufois, F., Vassas, C., Arnaud, M., 2010. In situ record of sedimentary processes near the Rhône River mouth during winter events (Gulf of Lions, Mediterranean Sea). Cont. Shelf Res. 30 (9), 1095–1107.

Marsaleix, P., Auclair, F., Floor, J.W., Herrmann, M.J., Estournel, C., Pairaud, I., Ulses, C., 2008. Energy conservation issues in sigma-coordinate free-surface ocean models. Ocean Model. 20, 61–89. https://doi.org/10.1016/j.ocemod.2007.07.005

Marsaleix, P., Michaud, H., Estournel, C., 2019. 3D phase-resolved wave modelling with a non-hydrostatic ocean circulation model. Ocean Modelling, doi : 10.1016/j.ocemod.2019.02.002

Martín, J., Durrieu de Madron, X., Puig, P., Bourrin, F., Palanques, A., Houpert, L., Higueras, M., Sanchez-Vidal, A., Calafat, A.M., Canals, M., Heussner, S., Delsaut, N., Sotin, C., 2013. Sediment transport along the Cap de Creus Canyon flank during a mild, wet winter. Biogeosciences 10, 3221–3239. http://dx.doi.org/10.5194/bg-10-3221-2013.

Mengual, B., Le Hir, P. , Cayocca, F., Garlan, T., 2017. Modelling Fine Sediment Dynamics: Towards a Common Erosion Law for Fine Sand, Mud and Mixtures. Water, 9, 564; doi:10.3390/w9080564

Michaud, H., Marsaleix, P., Leredde, Y., Estournel, C., Bourrin, F., Lyard, F., Mayet, C., Ardhuin, F., 2012. Three-dimensional modelling of wave-induced current from the surf zone to the inner shelf. Ocean Sci. 8, 657–681. https://doi.org/10.5194/os-8-657-2012

Mikolajczak, G., Ulses, C., Estournel, C., Bourrin, F., Pairaud, I., Martín, J., Puig, P., Durrieu de Madron, X., Leredde, Y., Marsaleix, P., 2020. Impact of storms on residence times and export of coastal waters during a mild fall/winter period in the Gulf of Lion. Continental Shelf Research 207, 104192. https://doi.org/10.1016/j.csr.2020.104192

Miralles, J., Radakovitch, O., Aloisi, J.-C., 2005. ^{210}Pb sedimentation rates from the Northwestern Mediterranean margin. Mar. Geol. 216 (3), 155–167.

Ody, A., Doxaran, D., Vanhellemont, Q., Nechad, B., Novoa, S., Many, G., Bourrin, F., Verney, R., Pairaud, I., Gentili, B., 2016. Potential of high spatial and temporal ocean color satellite data to study the dynamics of suspended particles in a micro-tidal river plume. Remote Sens. 8. doi: 10.3390/rs8030245.

Palanques, A., Garcia-Ladona, E., Gomis, D., Martín, J.,Marcos, M., Pascual, A., Puig, P., Emelianov, M., Guillen, J., Gili, J.M., Tintoré, J., Jordi, A., Basterretxea, G., Font, J., Segura, M., Blasco, D., Monserrat, S., Ruiz, S., Pages, F., 2005. General patterns of circulation, sediment fluxes and ecology of the Palamos (La Fonera) submarine canyon, North-western Mediterranean. Progress in Oceanography 66,89–119.

Palanques, A., Guillén, J., Puig, P., Durrieu de Madron, X., 2008. Storm-driven shelf- to-canyon suspended sediment transport at the southwestern Gulf of Lions. Cont. Shelf Res. 28, 1947–1956. http://dx.doi.org/10.1016/j.csr.2008.03.020

Palanques, A., Puig, P., Durrieu de Madron, X., Sanchez-Vidal, A., Pasqual, C., Martín, J., Calafat, A., Heussner, S., Canals, M., 2012. Sediment transport to the deep canyons and open-slope of the western Gulf of Lions during the 2006 intense cascading and open-sea convection period. Progress in Oceanography 106, 1–15.

Palanques, A., Puig, P., 2018. Particle fluxes induced by benthic storms during the 2012 dense shelf water cascading and open sea convection period in the northwestern Mediterranean basin. Marine Geology 406, 119–131. https://doi.org/10.1016/j.margeo.2018.09.010

Petrenko, A., Dufau, C., Estournel, C., 2008. Barotropic eastward currents in the western Gulf of Lion, north-western Mediterranean Sea, during stratified conditions. J. Mar. Syst. 74, 406–428. https://doi.org/10.1016/j.jmarsys.2008.03.004

Pont, D., Simonnet, J.P., Walter, A.V., 2002. Medium-term changes in suspended sediment delivery to the ocean: consequences of catchment heterogeneity and river management (Rhône River, France). Estuar. Coast. Shelf Sci. 54 (1), 1–18. https://doi.org/10.1006/ecss.2001.0829

Poulier, G., Launay, M., Le Bescond, C., Thollet, F., Coquery, M., Le Coz, J., 2019. Combining flux monitoring and data reconstruction to establish annual budgets of suspended particulate matter, mercury and PCB in the Rhône River from Lake Geneva to the Mediterranean Sea. Science of the Total Environment 658, 457–473

Provansal, M., Dufour, S., Sabatier, F., Anthony, E.J., Raccasi, G., Robresco, S., 2014. The geomorphic evolution and sediment balance of the lower Rhône River (southern France) over the last 130years: Hydropower dams versus other control factors. Geomorphology 219, 27-41, https://doi.org/10.1016/j.geomorph.2014.04.033

Puig, P., Palanques, A., Orange, D., Lastras, G., Canals, M., 2008. Dense shelf water cascades and sedimentary furrow formation in the Cap de Creus Canyon, northwestern Mediterranean Sea. Continent. Shelf Res. 28, 2017–2030. https://doi.org/10.1016/j.csr.2008.05.002

Puig, P., Durrieu de Madron, X., Salat, J., Schroeder, K., Martin, J., Karageorgis, A.P., Palanques, A., Roullier, F., Lopez-Jurado, J.L., Emelianov, M., Moutin, T., Houpert, L., 2013. Thick bottom nepheloid layers in the western Mediterranean generated by deep dense shelf water cascading. Progress in Oceanography 111, 1-23.

Radakovitch, O., Charmasson, S., Arnaud, M., Bouisset, P., 1999. ^{210}Pb and Caesium Accumulation in the Rhône Delta Sediments, Estuarine, Coastal and Shelf Science, 48, 77-92, https://doi.org/10.1006/ecss.1998.0405.

Ribó, M., Puig, P., Palanques, A., Lo Iacono, C., 2011. Dense shelf water cascades in the Cap de Creus and Palamós submarine canyons during winters 2007 and 2008. Marine Geology, Volume 284, Issues 1–4, 175-188. https://doi.org/10.1016/j.margeo.2011.04.001

Roussiez, V., Aloisi, J.C., Monaco, A., Ludwig, W., 2005. Early muddy deposits along the Gulf of Lions shoreline: A key for a better understanding of land-to-sea transfer of sediments and associated pollutant fluxes. Marine Geology 222 – 223 (2005) 345 – 358.

Sabatier, F., Maillet, G., Provansal, M., Fleury, T.-J., Suanez, S., Vella, C., 2006. Sediment budget of the Rhône delta shoreface since the middle of the 19th century. Marine Geology 234, 143 – 157. doi:10.1016/j.margeo.2006.09.022

Sadaoui, M., Ludwig, W., Bourrin, F., Raimbault, P., 2016. Controls, budgets and variability of riverine sediment fluxes to the Gulf of Lions (NW Mediterranean Sea). J. Hydrol. 540, 1002–1015. https://doi.org/10.1016/j.jhydrol.2016.07.012

Sanchez-Vidal, A., Llorca, M., Farré, M., Canals, M., Barceló, D., Puig, P., Calafat, A., 2015. Delivery of unprecedented amounts of perfluoroalkyl substances towards the deep-sea. Science of The Total Environment, 526,, 41-48, https://doi.org/10.1016/j.scitotenv.2015.04.080

Soulsby, R. Dynamics of Marine Sands: A Manual for Practical Applications; Thomas Telford: London, UK, 1997.

Soulsby, R.L. and Clarke, S., 2005. Bed shear-stress under combined waves and currents on smooth and rough beds (TR 137). Technical Report. HR Wallingford, Wallingford.

Thill, A., Moustier, S., Garnier, J.M., Estournel, C., Naudin, J.J., Bottero, J.Y., 2001. Evolution of particle size and concentration in the Rhône river mixing zone: influence of salt flocculation, Continental Shelf Research 21, 18–19, 2127-2140, https://doi.org/10.1016/S0278-4343(01)00047-4.

Thollet, F., Le Bescond, C., Lagouy, M., Gruat A., Grisot, G., Le Coz, J., Coquery, M., Lepage, H., Gairoard, S., Gattacceca, J.C., Ambrosi, J.-P., Radakovitch, O., Dur, G., Richard, L., Giner, F., Eyrolle, F., Angot, H., Mourier, D., Bonnefoy, A., Dugué, V., Launay, M., Troudet, L., Labille, J., Kieffer, L. , 2021. Observatoire des Sédiments du Rhône; INRAE. https://dx.doi.org/10.17180/OBS.OSR

Tolman, H.L., others, 2009. User Manual and System Documentation of WAVEWATCH III TM Version 3.14. Technical Note. MMAB Contribution 276.

Tramblay, Y., Somot, S. Future evolution of extreme precipitation in the Mediterranean. Climatic Change 151, 289–302 (2018). https://doi.org/10.1007/s10584-018-2300-5

Ulses, C., Estournel, C., Durrieu de Madron, X., Palanques, A., 2008a. Suspended sediment transport in the Gulf of Lions (NW Mediterranean): impact of extreme storms and floods. Cont. Shelf Res.

28, 2048–2070. http://dx.doi.org/10.1016/j.csr.2008.01.015

Ulses, C., Estournel, C., Puig, P., Durrieu de Madron, X., Marsaleix, P., 2008b. Dense water cascading in the northwestern Mediterranean during the cold winter 2005. Quantification of the export through the Gulf of Lion and the Catalan margin. Geophys. Res. Lett. 35, L07610. http://dx.doi.org/10.1029/2008GL033257

Ulses, C., Estournel, C., Bonnin, J., Durrieu de Madron, X., Marsaleix, P., 2008c. Impacts between storms and dense water cascading on shelf-slope exchange in the Gulf of Lions (NW Mediterranean). J. Geophys. Res. 113, C02010. http://dx.doi.org/10.1029/2006JC003795

Declaration of interests

☒ The authors declare that they have no known competing financial interests or personal relationships that could have appeared to influence the work reported in this paper.

☐ The authors declare the following financial interests/personal relationships which may be considered as potential competing interests:

Sediment dynamics in the Gulf of Lion (NW Mediterranean Sea) during two autumn-winter periods with contrasting meteorological conditions

Highlights

- Strong interannual variability of the sediment dynamics in the Gulf of Lion
- Massive sediment accumulation near the Rhone River mouth (~ 56% of the river inputs)
- Sediment deficit on the inner shelf due to the long-term reduction of the Rhone inputs
- Storm-induced sediment accumulation in the southwestern Gulf of Lion
- Cold winters mainly impact the southwestern and outer shelf and the submarine canyons